Information Sciences 596 (2022) 501–519

Contents lists available at ScienceDirect

Information Sciences

journal homepage: www.elsevier.com/locate/ins

Analysis of Turing patterns and amplitude equations in general forms under a reaction–diffusion rumor propagation system with Allee effect and time delay

Junlang Hu, Linhe Zhu *, Miao Peng

School of Mathematical Sciences, Jiangsu University, Zhenjiang 212013, PR China

ARTICLE INFO

Article history:
Received 18 November 2021
Received in revised form 12 February 2022
Accepted 6 March 2022
Available online 11 March 2022

Keywords:
Rumor propagation
Turing pattern
Amplitude equation
Reaction–diffusion system
Time delay

ABSTRACT

In this paper, we divide the population into three groups: susceptible individuals (S), infectious individuals (I) and removed individuals (R), and propose a rumor propagation dynamic model with Allee effect and cross-diffusion. Next, we have analyzed a general form of cross-diffusion model with time delay, and drawn a general conclusion of linear stability analysis of Turing bifurcation. However, Turing bifurcation analysis cannot give the specific shapes of the patterns under certain conditions. With the help of the "Multiple Scale Analysis" method, we derive the expression of the amplitude equation for the general form of weakly nonlinear models. Finally, we apply the above theorems to the analysis of our previously proposed model, and derive the appearance condition of the Turing bifurcation and the expression of the amplitude equation respectively. Through the numerical simulations, we have verified the correctness of the above theoretical analysis.

1. Introduction

Since Deley and Kendall established the first DK model in 1965 [9], researches about the classic rumor propagation systems started. The dynamics of rumor spreading has led to continuous research. In the 21st century, with the rise of the Internet, the spreading forms of rumors has become more diversified from the original way by mouth. With the advent of social media platforms such as Twitter and Facebook, people are able to receive various kinds of information all the time, including harmful rumors. Therefore, in the current context, modeling rumors propagation process with the aid of dynamic models has more practical meaning for predicting, preventing and finally controlling rumors. In 2015, Laarabi et al. [16] proposed an innovative rumor propagation system with latent and constant recruitment based on classic dynamics theory and analysis methods. Xiao et al. [29] further considered the influence of anti-rumor information and user's psychological factors on the spread of rumors. Liu et al. [24] divided the population into four categories: Rumor-Neutral, Rumor-Received, Rumor-Believed and Rumor-Denied, and performed more detailed modeling. Recent work in this area included Abta et al. [1], Cheng et al. [7]. Due to the similarity between the complex network structure and the Internet, in recent years, some scholars have transplanted the dynamic process of rumor spreading into the network models and made outstanding achievements, including Yu et al.[31], Li et al. [19], Jain et al. [14], Chen et al. [6] and Zhu et al. [36]. In 2019, Zhu et al. [32] proposed a SIS epidemic

* Corresponding author.
E-mail address: zlhnuaa@126.com (L. Zhu).

https://doi.org/10.1016/j.ins.2022.03.044
0020-0255/

model with nonlinear incidence rate and time lag on complex networks, and studied its properties with the aid of stability analysis theory and numerical simulation. Yu et al. [30] took into account the multilingual environment on the Internet, and proposed a I2SR rumor propagation model based on heterogeneous networks. They also verified their model with real data on Sina Weibo. When the reaction–diffusion terms are added to the above model, we can examine the dynamics of rumor propagation in the spatial dimension. In 2013, Lei et al. [17] investigated a free boundary problem on a reaction diffusion system for rumor spreading. They also gave the asymptotic spreading speed. Similar work on this aspect also includes Li and Ma [18], Zhu and Liu [34], Zhu et al. [35], and Huang et al. [13].

Under certain conditions, the reaction–diffusion system will lose stability in the spatial dimension because of the presence of the perturbation terms, and resulting in a pattern of spatial stationary state. This phenomenon can be used to explain the formation of patterns on the body surface of many organisms in nature. In 1952, Turing proposed the mechanism of this phenomenon in his paper "The Chemical Basis of Morphogenesis" [28]. Turing's theorem has been applied to many infectious disease models and biological population models. Chang et al. [4] applied the above theory to the SIR infectious disease model in the context of complex networks, and considered the impact of cross-diffusion to pattern formation. Tao et al. [27] investigated the pattern under the combined influence of periodic disturbance and time delay in the predator–prey model. He et al. [12] innovatively applied the pattern dynamics model to the field of rumor propagation, and analyzed the dynamics of rumor propagation on networks such as "WS" and "BA". Zhu et al. [33] separated the reaction–diffusion model with terms containing only the time-delay and no time-delay, then they put forward the general conclusion for the occurrence of Turing bifurcation, which had a great pioneering value. It provides convenience for other scholars' research in the future. On the basis of their work, this paper further explores the existence conditions of the Turing bifurcation in the more general case where the reaction–diffusion equation cannot be divided into the addition of time-delay terms and non-time-delay terms, and a proof is given.

The above work uses bifurcation theory to study the appearance conditions of patterns. Bifurcation analysis is a necessary tool to explain the formation of pattern and nonlinear dynamic behavior in the reaction diffusion process, but it still has defects. It cannot accurately explain the shape of the pattern generated under certain conditions. The amplitude equation theory proposed by Newell and Whitehead [25] can do just that. The amplitude equation theory states that an ideal pattern without any defects near the bifurcation points of the system can be described by the linear combination of oscillating wave vectors, so that the shapes of the patterns can be precisely predicted. Chen et al. [5], Banerjee et al. [3], Liu et al. [21], Guo et al. [11], Gan et al. [10], Liu et al. [23]. used the amplitude equation to explain the Turing pattern formation process of the reaction–diffusion system. It is worth mentioning that although the calculation is complicated, the theory of the amplitude equation is relatively fixed. So it is possible to use a mechanized method for calculation as long as the in general theory of the amplitude equation is derived. The article by Li et al. [20] completed the derivation of the general formula theory of the amplitude equation of the general weakly nonlinear system but had some small imperfections. Liu and Wang [22] used the "Norm Form Method" to derive the amplitude equation, and gave an algorithm program for mechanized calculation using Maple. On the basis of their work, this paper continues to propose a more completed general formula conclusion that uses multiple scale analysis to derive the amplitude equation of the general form. Hoping our work is able to facilitate the derivation and calculation of future researchers.

The structure of this article is organized as follows: In Section 2, we propose a rumor propagation dynamic model with Allee effect and the cross-diffusion term. In Section 3, we draw a general conclusion of linear stability analysis of Turing bifurcation in presence of time delay. In Section 4, we will derive the general form of the amplitude equation for the general weakly nonlinear systems, and apply the theory to the model proposed in Section 2. In Section 5, we carry out the numerical simulations to verify the above conclusions. In Section 6, we summarize the work of this article.

2. Modelling

Since Turing's pioneering work in 1952, "pattern dynamics" has become a very active research field. It can reflect the structural changes between various elements in the dynamic reaction–diffusion system and is applied in various aspects of physics, chemistry, and biology. A non-linear system is asymptotically stable when there is no diffusion, but becomes unstable when the diffusion is presented. This phenomenon is called Turing instability. It was found that the formation of Turing patterns has the following biological mechanism:

- Two substances, "activator" and "blocker" must coexist in the system, which will accelerate and slow down the rate of reaction–diffusion process respectively.
- The diffusion rate of "activator" is far lower than that of "blocker".

A reaction–diffusion system like that may amplify small perturbations, and form a spatially stable pattern. For more detailed description of this biological mechanism, please see Ouyang Qi's book [26]. The Turing instability analysis of the dynamic system has been applied to many infectious disease models and biological population models. This paper mainly focuses its application to the dynamic model of rumor propagation.

To establish our model, we divide people into three groups on networks:

- $S(t,x)$ (the susceptible individuals). People who have not be exposed to the rumor but have the chance to become the rumor-spreading individuals.
- $I(t,x)$ (the infectious individuals). People who have believed the rumor and are able to infect susceptible individuals.
- $R(t,x)$ (the removed individuals). People who used to be rumor-believers but have already realized that the rumor is fake and will no longer believe it.

Under the previous grouping case, we propose the following continuous reaction–diffusion rumor propagation model (1) with Allee effect and time delay.

$$\begin{cases} \frac{\partial S(t,x)}{\partial t} = d_{11}\Delta S + d_{12}\Delta I + rS\left(1-\frac{S(t-\tau,x)}{K}\right)\left(\frac{S}{A}-1\right) - \beta SI^2,\ t>0,\ x\in\Omega, \\ \frac{\partial I(t,x)}{\partial t} = d_{12}\Delta S + d_{22}\Delta I + \beta SI^2 - \mu I^2,\ t>0,\ x\in\Omega, \\ \frac{\partial S}{\partial n}\big|_{\partial\Omega} = \frac{\partial I}{\partial n}\big|_{\partial\Omega} = 0,\ t\geqslant 0,\ x\in\partial\Omega, \\ S(t,x) = S_0(\theta,x)\geqslant 0, I(t,x) = I_0(\theta,x)\geqslant 0,\ \theta\in[-\tau,0],\ x\in\Omega. \end{cases} \tag{1}$$

We introduce of a time delay τ which represents the delay of the environment's curbing effect on the growth of the susceptible population (shorted to S below). In this model, the meanings of all terms are as follows:

- $rS\left(1-\frac{S(t-\tau)}{K}\right)\left(\frac{S}{A}-1\right)$. r is the inherent growth rate of S population. K is the maximum carrying capacity of the information network, and the delay term τ reflects the delayed influence from network environment for the increase in population. It is found in nature that as the population of a specie increases, cooperation and links among individuals will also get strengthened so that the population can survive and reproduce better. Allee effect describes the positive correlation between density and average fitness of some species. This conception was first put forward by Allee in his researches about goldfish [2] (1932). The Allee effect is added to the model, where A is the critical space carrying capacity of S.
- βSI^2. β is the probability of contact infection, the high-order exposure saturation is applied here.
- μI^2. μ is the removal rate. The term indicates the process that two rumor spreaders have become disconvinced of the rumor after communicating.
- $d_{11}\Delta S$ and $d_{22}\Delta I$. The self-diffusion terms of the reaction–diffusion system. They represent the spatial movement inside S and I groups, where $d_{11}, d_{22} > 0$ are the self-diffusion coefficients, and $\Delta = \frac{\partial^2}{\partial x^2} + \frac{\partial^2}{\partial y^2}$ is the Laplace operator.
- $d_{12}\Delta I$ and $d_{21}\Delta S$. The cross-diffusion terms of the reaction–diffusion system. $d_{12}\Delta I$ represents the flow process of S to low-density areas of the I population, $d_{21}\Delta S$ represents its inverse.

3. Turing bifurcation analysis

3.1. Stability analysis around the equilibrium point

In this part, we consider the situation of uniform space, where the perturbation coefficients are zero. In the case of no disturbance and no time delay, let the perturbation-terms' coefficients be zero in system (1), and consider the left side of the system be zero, we have

$$\begin{cases} \left[rS(1-\frac{S}{K})(\frac{S}{A}-1) - \beta SI^2\right]\Big|_{S=S^*,\ I=I^*} = 0, \\ \left[\beta SI^2 - \mu I^2\right]\Big|_{S=S^*,\ I=I^*} = 0. \end{cases} \tag{3.1}$$

By solving it we obtain that if $(C1)$ $\beta A < \mu < \beta K$ holds, then

$$\begin{cases} S^* = \frac{\mu}{\beta}, \\ I^* = \sqrt{\frac{r}{\beta}\left(1-\frac{\mu}{\beta K}\right)\left(\frac{\mu}{\beta A}-1\right)}. \end{cases} \tag{3.2}$$

So we have the rumor-spreading equilibrium point $E^* = (S^*, I^*) = \left(\frac{\mu}{\beta}, \sqrt{\frac{r}{\beta}\left(1-\frac{\mu}{\beta K}\right)\left(\frac{\mu}{\beta A}-1\right)}\right)$. In addition, system (1) has the zero equilibrium point $E_1^* = (0,0)$, and the rumor-free equilibrium points $E_2^* = (K,0), E_3^* = (A,0)$. We mainly study the situation that rumors appear in the initial state, so in this article we do not consider those equilibrium points E_1^*, E_2^* and E_3^*.

We perform stability analysis near the rumor-spreading equilibrium E^* when $\tau = 0$. The Jacobian matrix J of system (1) at the rumor-spreading equilibrium is

$$J|_{E^*} \equiv \begin{pmatrix} a_{11} & a_{12} \\ a_{21} & a_{22} \end{pmatrix}\Big|_{E^*} = \begin{pmatrix} \frac{\partial F}{\partial S} & \frac{\partial F}{\partial I} \\ \frac{\partial G}{\partial S} & \frac{\partial G}{\partial I} \end{pmatrix}\Big|_{E^*} = \begin{pmatrix} -\frac{3rS^{*2}}{AK} + 2rS^*\left(\frac{1}{A}+\frac{1}{K}\right) - r - \beta I^{*2} & -2\beta S^*I^* \\ \beta I^{*2} & 2\beta S^*I^* - 2\mu I^* \end{pmatrix}, \tag{3.3}$$

where

$$F(S,I)=rS\left(1-\frac{S}{K}\right)\left(\frac{S}{A}-1\right)-\beta SI^2,\ G(S,I)=\beta SI^2-\mu I^2.$$

Substituting the expression of S^* and I^* into entries of Jacobian matrix, we obtain

$$\begin{aligned}
&a_{11}=\tfrac{r\mu}{KA\beta^2}[\beta(A+K)-2\mu],\\
&a_{12}=-2\mu\sqrt{\tfrac{r}{\beta}\left(1-\tfrac{\mu}{\beta K}\right)\left(\tfrac{\mu}{\beta A}-1\right)},\\
&a_{21}=r\left(1-\tfrac{\mu}{\beta K}\right)\left(\tfrac{\mu}{\beta A}-1\right),\quad a_{22}=0.
\end{aligned}\tag{3.4}$$

The theorem describing the stability conditions of system (1) is proposed in the following.

Theorem 3.1. *Under the condition* (C1)*, there exists one and only one rumor-spreading equilibrium point* E^**. Select* μ *as the control parameter, and define* $\mu_{t_1}=\beta(A+K)/2$*. If* $\mu>\mu_{t_1}$*,* E^* *is locally asymptotically stable. The Hopf bifurcation appears when* $\mu=\mu_{t_1}$*, and further the system lose stability in space dimension if* $\mu<\mu_{t_1}$*.*

Proof. According to Ruth-Hurwitz's criterion, the rumor-spreading equilibrium point is locally asymptotically stable if $a_{11}+a_{22}<0$ and $a_{11}a_{22}-a_{12}a_{21}>0$. Since

$$a_{11}a_{22}-a_{12}a_{21}=2\mu\sqrt{\frac{r}{\beta}\left(1-\frac{\mu}{\beta K}\right)\left(\frac{\mu}{\beta A}-1\right)}\cdot r\left(1-\frac{\mu}{\beta K}\right)\left(\frac{\mu}{\beta A}-1\right)>0,\tag{3.5}$$

we only have to ensure that $a_{11}+a_{22}=-\frac{2r\mu^2}{KA\beta}+\frac{r\mu}{\beta}\left(\frac{1}{A}+\frac{1}{K}\right)<0$, which is equivalent to $\mu>\mu_{t_1}:=\beta(A+K)/2$.

3.2. Turing bifurcation analysis

We put forward the following theorem to describe the general occurrence condition for Turing bifurcation of a reaction–diffusion model with time delay.

Theorem 3.2. *For a reaction–diffusion system with time delay in a general form*

$$\begin{cases}\frac{\partial S(t,x)}{\partial t}=F(S(t,x),I(t,x),S(t-\tau,x),I(t-\tau,x))+d_{11}\Delta S+d_{12}\Delta I,\\ \frac{\partial I(t,x)}{\partial t}=G(S(t,x),I(t,x),S(t-\tau,x),I(t-\tau,x))+d_{11}\Delta S+d_{12}\Delta I.\end{cases}\tag{3.6}$$

By making linear approximation, the following matrix can be obtained as

$$\begin{pmatrix}\lambda m_{11}-\left(a_{11}-k^2d_{11}\right) & \lambda m_{12}-\left(a_{12}-k^2d_{12}\right)\\ \lambda m_{21}-\left(a_{21}-k^2d_{21}\right) & \lambda m_{22}-\left(a_{22}-k^2d_{22}\right)\end{pmatrix}\Bigg|_{E^*}\begin{pmatrix}\widetilde{S}\\ \widetilde{I}\end{pmatrix}=0,\tag{3.7}$$

where

$$\begin{aligned}
&m_{11}=1+\tau\tfrac{\partial F}{\partial S(t-\tau)}\Big|_{\tau=0},\quad m_{12}=\tau\tfrac{\partial F}{\partial I(t-\tau)}\Big|_{\tau=0},\\
&m_{21}=\tau\tfrac{\partial G}{\partial S(t-\tau)}\Big|_{\tau=0},\qquad m_{22}=1+\tau\tfrac{\partial G}{\partial I(t-\tau)}\Big|_{\tau=0}.
\end{aligned}\tag{3.8}$$

The corresponding characteristic equation is

$$\begin{aligned}
&\lambda^2-C_k\lambda+D_k=0,\\
&C_k=\left(\tfrac{1}{m_{11}m_{22}-m_{12}m_{21}}\cdot\left[\left(a_{22}-k^2d_{22}\right)m_{11}+\left(a_{11}-k^2d_{11}\right)m_{22}-\left(a_{21}-k^2d_{21}\right)m_{12}-\left(a_{12}-k^2d_{12}\right)m_{21}\right]\right)\Big|_{E^*},\\
&D_k=\left(\tfrac{1}{m_{11}m_{22}-m_{12}m_{21}}\cdot\left[(d_{11}d_{22}-d_{12}d_{21})k^4-(a_{11}d_{22}+a_{22}d_{11}-a_{12}d_{21}-a_{21}d_{12})k^2+\det(J)\right]\right)\Big|_{E^*}.
\end{aligned}\tag{3.9}$$

Proof. For system (3.6), we can use the following linear approximation formula

$$S(t-\tau)\approx S(t)-\frac{\partial S}{\partial t}\cdot\tau,\quad I(t-\tau)\approx I(t)-\frac{\partial I}{\partial t}\cdot\tau.\tag{3.10}$$

Expand it around $\tau=0$, we obtain

$$\begin{aligned} F &= F|_{\tau=0} + \tau\frac{dF}{d\tau}\Big|_{\tau=0} \\ &= F|_{\tau=0} + \tau\left(\frac{\partial F}{\partial S(t-\tau)}\cdot\frac{\partial S(t-\tau)}{\partial \tau} + \frac{\partial F}{\partial I(t-\tau)}\cdot\frac{\partial I(t-\tau)}{\partial \tau}\right)\Big|_{\tau=0} \\ &= F(S,I) - \tau\left(\frac{\partial F}{\partial S(t-\tau)}\cdot\frac{\partial S}{\partial t} + \frac{\partial F}{\partial I(t-\tau)}\cdot\frac{\partial I}{\partial t}\right)\Big|_{\tau=0}, \\ G &= G(S,I) - \tau\left(\frac{\partial G}{\partial S(t-\tau)}\cdot\frac{\partial S}{\partial t} + \frac{\partial G}{\partial I(t-\tau)}\cdot\frac{\partial I}{\partial t}\right)\Big|_{\tau=0}, \end{aligned} \tag{3.11}$$

where $F(S,I) = F(S,I,S(t-\tau),I(t-\tau))|_{\tau=0}$, $G(S,I) = G(S,I,S(t-\tau),I(t-\tau))|_{\tau=0}$. They have the same form with the expression derived by replacing all the $S(t-\tau)$, $I(t-\tau)$ terms with S, I in $F(S,I,S(t-\tau),I(t-\tau)), G(S,I,S(t-\tau),I(t-\tau))$. Replace Eq. (3.11) into the system and rearrange it to get the following equations

$$\begin{cases} m_{11}\frac{\partial S}{\partial t} + m_{12}\frac{\partial I}{\partial t} = F(S,I) + d_{11}\Delta S + d_{12}\Delta I, \\ m_{21}\frac{\partial S}{\partial t} + m_{22}\frac{\partial I}{\partial t} = G(S,I) + d_{21}\Delta S + d_{22}\Delta I, \end{cases} \tag{3.12}$$

where $m_{11}, m_{12}, m_{21}, m_{22}$ are defined in Eq. (3.8). Using the following formulas,

$$\begin{aligned} &\widetilde{S} = S^*\cdot e^{\lambda t}\cos(k_x x)\cos(k_y y), \widetilde{I} = I^*\cdot e^{\lambda t}\cos(k_x x)\cos(k_y y), \\ &S = S^* + \widetilde{S}, \quad I = I^* + \widetilde{I}, \quad \frac{\partial S}{\partial t} = \lambda\widetilde{S}, \ \frac{\partial I}{\partial t} = \lambda\widetilde{I}, \\ &\Delta S = \left(\frac{\partial^2}{\partial x^2} + \frac{\partial^2}{\partial y^2}\right)S = -\left(k_x^2 + k_y^2\right)\widetilde{S} := -k^2\widetilde{S}, \\ &\Delta I = \left(\frac{\partial^2}{\partial x^2} + \frac{\partial^2}{\partial y^2}\right)I = -\left(k_x^2 + k_y^2\right)\widetilde{I} := -k^2\widetilde{I}, \end{aligned} \tag{3.13}$$

by expanding the spatiotemporal perturbation on the Fourier space and ignoring the higher-order items, we get the following matrix

$$\begin{pmatrix} \lambda m_{11} - \left(a_{11} - k^2 d_{11}\right) & \lambda m_{12} - \left(a_{12} - k^2 d_{12}\right) \\ \lambda m_{21} - \left(a_{21} - k^2 d_{21}\right) & \lambda m_{22} - \left(a_{22} - k^2 d_{22}\right) \end{pmatrix}\Bigg|_{E^*} \begin{pmatrix} \widetilde{S} \\ \widetilde{I} \end{pmatrix} = 0. \tag{3.14}$$

Define matrices $D$and M as

$$D = \begin{pmatrix} d_{11} & d_{12} \\ d_{21} & d_{22} \end{pmatrix}, \quad M = \begin{pmatrix} m_{11} & m_{12} \\ m_{21} & m_{22} \end{pmatrix}\Big|_{E^*},$$

and let $|\lambda M - \left(J - k^2 D\right)| = 0$. So we obtain the characteristic equation of system (3.6), which is expressed in Eq. (3.9).

3.3. Analysis for system (1)

Theorem 3.3. *The necessary conditions for the emergence of Turing bifurcation in system (1) are* $(C1), (C2)$ $\mu > \mu_{t_1} = \frac{\beta(K+A)}{2}$ *and* $(C3)$ $\min\{D_k\} < 0$, $m_{11}|_{E^*} > 0$, $d_{11}d_{22} - d_{12}d_{21} > 0$, $a_{11}d_{22} - a_{12}d_{21} - a_{21}d_{12} > 0$.

Proof. In our model, $m_{11} = 1 - \tau\frac{rS}{K}\cdot\left(\frac{S}{A} - 1\right), m_{12} = m_{21} = 0, m_{22} = 1$. The coefficients of the corresponding characteristic equation are

$$\begin{aligned} C_k &= \left(\frac{1}{m_{11}}\cdot\left(-\frac{2r\mu^2}{KA\beta^2} + \frac{r\mu}{\beta}\left(\frac{1}{A} + \frac{1}{K}\right)\right) - k^2\left(d_{22} + \frac{1}{m_{11}}d_{11}\right)\right)\Big|_{E^*}, \\ D_k &= \left(\frac{1}{m_{11}}\cdot\left[(d_{11}d_{22} - d_{12}d_{21})k^4 - (a_{11}d_{22} - a_{12}d_{21} - a_{21}d_{12})k^2 + \det(J)\right]\right)\Big|_{E^*}. \end{aligned}$$

According to Ref. [20], the critical condition for the appearance of the Turing bifurcation is that

$$Im(\lambda_k) = 0, \quad Re(\lambda_k) = 0 \quad \text{at some } k = k_T \neq 0,$$

where $\lambda_k = \frac{1}{2}\left[C_k \pm \sqrt{C_k^2 - 4D_k}\right]$ is the root of characteristic equation. Hopf bifurcation occurs when

$$Im(\lambda_k) \neq 0, \quad Re(\lambda_k) = 0 \quad \text{at some } k = k_T = 0.$$

It can be assumed that the time delay τ is very small, as a result $m_{11} = 1 - \tau\frac{rS}{K}\cdot\left(\frac{S}{A} - 1\right) > 0$. The Hopf bifurcation appears when $\mu = \mu_{t_1}$. Further, the condition under which the Turing bifurcation emerges is in the following.

1. When $k = 0$, the system is stable:

$$\begin{cases} C_0 = \frac{r\mu}{m_{11}|_{E^*} KA\beta^2}[\beta(A+K) - 2\mu] < 0 \Rightarrow \mu > \mu_{t_1} = \frac{\beta(K+A)}{2}, \\ D_0 = \frac{1}{m_{11}|_{E^*}} \cdot \det(J) > 0. (\text{It is always true.}) \end{cases} \tag{3.15}$$

2. When $k \neq 0$, we consider the Turing instability caused by the violation of the condition "D_K constantly greater than or equal to 0" here. At this point the system should meet the condition of $(C3.1)$ $d_{11}d_{22} - d_{12}d_{21} > 0$ (meaning the cross-diffusion factors are smaller), so that D_k, the 4-order function of k, has the upwards direction. $(C3.2)$ $min\{D_k\} < 0 \Longleftrightarrow 4(d_{11}d_{22} - d_{12}d_{21})\det(J) - (a_{11}d_{22} - a_{12}d_{21} - a_{21}d_{12})^2 < 0$, and $m_{11}|_{E^*} > 0$ ensures the existence of Turing bifurcation. $(C3.3)$ $a_{11}d_{22} - a_{12}d_{21} - a_{21}d_{12} > 0$ should also be satisfied so that the minimum value of D_k can be obtained. Under those restrictions, the minimum value of D_k is smaller than 0 and Turing bifurcation appears. From (C3.2) and (C3.3), we get two critical values for $\mu : \mu_{t_2}, \mu_{t_3}$. Since their expressions are complicated, we cannot give a specific analytical formula for them, but we can use Matlab software to plot the image describing how the left side of the inequalities change with μ and solve it numerically.

We fix the values of variables at: $r = 0.1,\ K = 1,\ A = 0.3,\ \beta = 0.8,\ \tau = 0.1,\ d_{11} = 5.5,\ d_{12} = 0.7,\ d_{21} = 0.8,\ d_{22} = 0.2$. Then the conditions for the existence of Turing bifurcation are

$$\begin{cases} (C1) \quad 0.24 < \mu < 0.8, \\ (C2) \quad \mu > \mu_{t_1} = 0.52, \\ (C3) \quad \mu < \mu_{t_2} = 0.7924,\ \mu < \mu_{t_3} = 0.79631,\ d_{11}d_{22} - d_{12}d_{21} = 0.54 > 0. \end{cases} \tag{3.16}$$

The corresponding critical wave number of the system is $k_T = 0.1353$.

We plot images reflecting how D_k and the "real part of the largest eigenvalue" varying with the wave number k to verify the above conclusion. Let $\mu = 0.7900,\ 0.7952,\ 0.798$ respectively. It can be seen from Fig. 1a that the curve represented by the critical value μ_{t_2} just intersects the horizontal line $y = 0$ when k is equal to the critical wave number. If $\mu = 0.79 < \mu_{t_2}$, we have $\min\{D_k\} < 0$, then Turing bifurcation exists. When $\mu = 0.798 > \mu_{t_2}$, D_k is always positive and no Turing pattern can be found.

From Fig. 1b, we know that when $\mu = 0.79 < \mu_{t_2}$, the real part of the greater eigenvalue changes from a negative value to a positive value, which is consistent with the occurrence condition of the Turing bifurcation.

Numerical simulation under conditions deduced above will produce Turing pattern. However, we cannot determine the shape of the pattern under some certain condition. The amplitude equation is an effective tool to describe complex dynamic behavior of weakly nonlinear systems. Using "Multiple Scale Analysis" method to derive the amplitude equation near the critical value where the Turing bifurcation appears, the shape of patterns can be accurately obtained.

4. Weakly nonlinear analysis

In this section, we use the multiple-scale analysis method to derive the amplitude equation of the Turing pattern under the second-level perturbations. The multiple-scale analysis method was proposed by Newell and Whitehead in 1969 [25]. This theory states that an ideal pattern without any defects near the bifurcation points of the system can be described by the linear combination of oscillating wave vectors, so that the shapes of the patterns can be precisely predicted. Based on

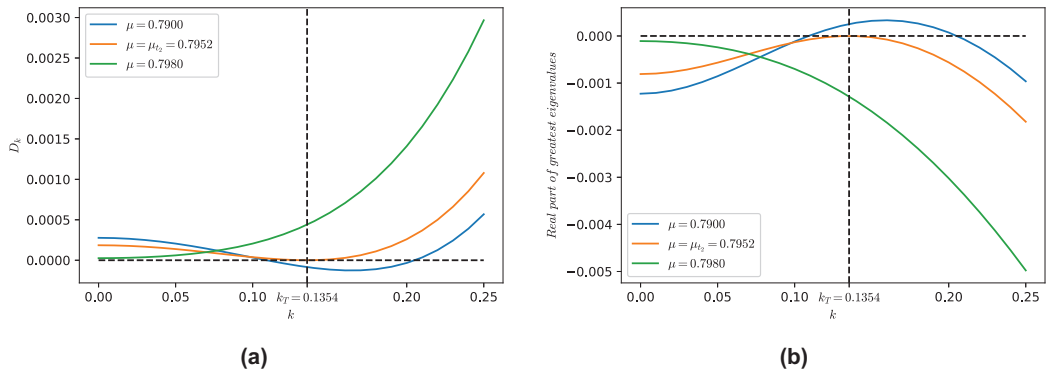

Fig. 1. Fig. 1a: D_k with wave number k, Fig. 1b: "real part of the largest eigenvalue" with wave number k. The value of μ in each curve in the figures are shown in the legends, and the values of other variables are fixed as: $r = 0.1,\ K = 1,\ A = 0.3,\ \beta = 0.8,\ \tau = 0.1,\ d_{11} = 5.5,\ d_{12} = 0.7,\ d_{21} = 0.8,\ d_{22} = 0.2$.

their theory as well as other people's work (Li et al. [20], Chen et al. [5], Banerjee et al. [3], Guo et al. [11], Gan et al. [10], Liu et al. [21], Liu et al. [23], Liu et al. [22]) on the amplitude equation of reaction–diffusion systems, we propose the following theorem.

4.1. The general form of the amplitude equation of reaction–diffusion system

Theorem 4.1. *For the reaction–diffusion system in the general form*

$$\frac{\partial \mathbf{U}}{\partial t} = T(\mathbf{U}) = L\mathbf{U} + NL(\mathbf{U}), \quad \mathbf{U} = \begin{pmatrix} u \\ v \end{pmatrix}, \quad T(\mathbf{U}) = \begin{pmatrix} f(u,v) \\ g(u,v) \end{pmatrix}, \tag{4.1}$$

the linear term is

$$L = L_T + (e_T - e)N = \begin{pmatrix} a_{11}^T + d_{11}\Delta & a_{12}^T + d_{12}\Delta \\ a_{21}^T + d_{21}\Delta & a_{22}^T + d_{22}\Delta \end{pmatrix} + (e_T - e)\begin{pmatrix} n_{11} & n_{12} \\ n_{21} & n_{22} \end{pmatrix}, \tag{4.2}$$

with

$$\begin{pmatrix} a_{11} & a_{12} \\ a_{21} & a_{22} \end{pmatrix} = \begin{pmatrix} \frac{\partial f}{\partial u} & \frac{\partial f}{\partial u} \\ \frac{\partial g}{\partial u} & \frac{\partial g}{\partial u} \end{pmatrix}\Big|_{E^*}, \quad a_{ij}^T = a_{ij}\Big|_{e=e_T}, \quad n_{ij} = -\frac{da_{ij}}{de}\Big|_{e=e_T}, \ (i,j=1,2). \tag{4.3}$$

In the above equations, we denote the controlling parameter as e, whose critical value is e_T. Note that all the a_{ij} that appear in this theorem are redefined in Eq. (4.3). In the amplitude equation, we want to study the effect of changing the control variable e on the shapes of the patterns while other parameters in the model remain unchanged. Therefore, e in the model is an unknown parameter at this time, and a_{ij} is not a constant but also an unknown parameter which has e in it. That is the reason that we redefine them.

Moreover, the nonlinear term can be expanded as

$$NL(\mathbf{U}) = \begin{pmatrix} f_{11}u^2 + f_{12}uv + f_{22}v^2 \\ g_{11}u^2 + g_{12}uv + g_{22}v^2 \end{pmatrix} + \begin{pmatrix} f_{111}u^3 + f_{112}u^2v + f_{122}uv^2 + g_{222}v^3 \\ g_{111}u^3 + g_{112}u^2v + g_{122}uv^2 + g_{222}v^3 \end{pmatrix} + O\left(\mathbf{U}^4\right), \tag{4.4}$$

where

$$\begin{aligned} \begin{pmatrix} f_{11} & f_{12} & f_{22} \\ g_{11} & g_{12} & g_{22} \end{pmatrix} &= \frac{1}{2}\begin{pmatrix} \frac{\partial^2 f}{\partial u^2} & 2\frac{\partial^2 f}{\partial u \partial v} & \frac{\partial^2 f}{\partial v^2} \\ \frac{\partial^2 g}{\partial u^2} & 2\frac{\partial^2 g}{\partial u \partial v} & \frac{\partial^2 g}{\partial v^2} \end{pmatrix}\Big|_{E^*}, \\ \begin{pmatrix} f_{111} & f_{112} & f_{122} & f_{222} \\ g_{111} & g_{112} & g_{122} & g_{222} \end{pmatrix} &= \frac{1}{6}\begin{pmatrix} \frac{\partial^3 f}{\partial u^3} & 3\frac{\partial^3 f}{\partial u \partial u \partial v} & 3\frac{\partial^3 f}{\partial u \partial v \partial v} & \frac{\partial^3 f}{\partial v^3} \\ \frac{\partial^3 g}{\partial u^3} & 3\frac{\partial^3 g}{\partial u \partial u \partial v} & 3\frac{\partial^3 g}{\partial u \partial v \partial v} & \frac{\partial^3 g}{\partial v^3} \end{pmatrix}\Big|_{E^*}. \end{aligned} \tag{4.5}$$

The critical value of controlling parameter e_T can be derived by solving the equation $\min\{D_k\} = 0$. The general form of D_k in a reaction–diffusion system has been described in Eq. (3.9). Let $k_T^2 = \sqrt{\frac{\det(J)}{d_{11}d_{22} - d_{12}d_{21}}}\Big|_{e=e_T}$, and define

$$\varphi = -\frac{a_{12}^T - d_{12}k_T^2}{a_{11}^T - d_{11}k_T^2} = -\frac{a_{22}^T - d_{22}k_T^2}{a_{21}^T - d_{21}k_T^2}, \quad \psi = -\frac{a_{11}^T - d_{11}k_T^2}{a_{21}^T - d_{21}k_T^2} = -\frac{a_{12}^T - d_{12}k_T^2}{a_{22}^T - d_{22}k_T^2}.$$

The amplitude equation of reaction–diffusion system (4.1) under the first-level perturbation is

$$\begin{cases} (\varphi + \psi)\frac{\partial W_1}{\partial T_1} = e_1[(n_{11}\varphi + n_{12}) + \psi(n_{21}\varphi + n_{22})]W_1 + (I_1 + \psi I_2)2\overline{W}_2\overline{W}_3, \\ (\varphi + \psi)\frac{\partial W_2}{\partial T_1} = e_1[(n_{11}\varphi + n_{12}) + \psi(n_{21}\varphi + n_{22})]W_2 + (I_1 + \psi I_2)2\overline{W}_1\overline{W}_3, \\ (\varphi + \psi)\frac{\partial W_3}{\partial T_1} = e_1[(n_{11}\varphi + n_{12}) + \psi(n_{21}\varphi + n_{22})]W_3 + (I_1 + \psi I_2)2\overline{W}_1\overline{W}_2. \end{cases} \tag{4.6}$$

where

$$I_1 = f_{11}\varphi^2 + f_{12}\varphi + f_{22}, \quad I_2 = g_{11}\varphi^2 + g_{12}\varphi + g_{22}.$$

In addition, the amplitude equation of system (4.1) under the second-level perturbation has the following form

$$\begin{cases} \tau_0\frac{\partial A_1}{\partial t} = \eta A_1 + h\overline{A}_2\overline{A}_3 - \left[g_1|A_1|^2 + g_2\left(|A_2|^2 + |A_3|^2\right)\right]A_1, \\ \tau_0\frac{\partial A_2}{\partial t} = \eta A_2 + h\overline{A}_1\overline{A}_3 - \left[g_1|A_2|^2 + g_2\left(|A_1|^2 + |A_3|^2\right)\right]A_2, \\ \tau_0\frac{\partial A_3}{\partial t} = \eta A_3 + h\overline{A}_1\overline{A}_2 - \left[g_1|A_3|^2 + g_2\left(|A_1|^2 + |A_2|^2\right)\right]A_3. \end{cases} \tag{4.7}$$

where

$$\tau_0=\frac{\varphi+\psi}{e_TQ},\quad \eta=\frac{e_T-e}{e_T},\quad h=\frac{2(I_1+\psi I_2)}{e_TQ},g_1=-\frac{G_1}{e_TQ},\quad g_2=-\frac{G_2}{e_TQ}, \tag{4.8}$$

with

$$\begin{aligned}
&Q=(\varphi n_{11}+n_{12})+\psi(\varphi n_{21}+n_{22}),\\
&G_1=(u_{00}+u_{11})(H_1+\psi H_2)+(v_{00}+v_{11})(H_3+\psi H_4)+3(R_1+\psi R_2),\\
&G_2=(u_{00}+u_{22})(H_1+\psi H_2)+(v_{00}+v_{22})(H_3+\psi H_4)+6(R_1+\psi R_2),\\
&H_1=2f_{11}\varphi+f_{12},\quad H_2=2g_{11}\varphi+g_{12},\quad H_3=2f_{22}+f_{12}\varphi,\quad H_4=2g_{22}+g_{12}\varphi,\\
&R_1=f_{111}\varphi^3+f_{112}\varphi^2+f_{122}\varphi+f_{222},\quad R_2=g_{111}\varphi^3+g_{112}\varphi^2+g_{122}\varphi+g_{222}.
\end{aligned}$$

and

$$\begin{pmatrix}u_{00}\\v_{00}\end{pmatrix}=-2L_T^{-1}\begin{pmatrix}I_1\\I_2\end{pmatrix},\quad \begin{pmatrix}u_{11}\\v_{11}\end{pmatrix}=-\left(L_T-4k_T^2D\right)^{-1}\begin{pmatrix}I_1\\I_2\end{pmatrix},\quad \begin{pmatrix}u_{22}\\v_{22}\end{pmatrix}=-2\left(L_T-3k_T^2D\right)^{-1}\begin{pmatrix}I_1\\I_2\end{pmatrix}.$$

Proof. By expanding the original reaction–diffusion system with Taylor's formula up to the third order, and tearing apart the linear terms and the nonlinear terms, it is easy to obtain system (4.1) above. The forms of the linear terms are described in (4.2), and the nonlinear terms are described in (4.4).

Expanding the model further by using

$$\begin{cases}U=\varepsilon\begin{pmatrix}u_1\\v_1\end{pmatrix}+\varepsilon^2\begin{pmatrix}u_2\\v_2\end{pmatrix}+\varepsilon^3\begin{pmatrix}u_3\\v_3\end{pmatrix}+o(\varepsilon^3),\\ NL(\mathbf{U})=\varepsilon^2n_2+\varepsilon^3n_3+o(\varepsilon^3),\\ e_T-e=\varepsilon e_1+\varepsilon^2e_2+\varepsilon^3e_3+o(\varepsilon^3),\end{cases} \tag{4.9}$$

with

$$\begin{aligned}
n_2&=\begin{pmatrix}f_{11}u_1^2+f_{12}u_1v_1+f_{22}v_1^2\\ g_{11}u_1^2+g_{12}u_1v_1+g_{22}v_1^2\end{pmatrix},\\
n_3&=\begin{pmatrix}2f_{11}u_1u_2+f_{12}(u_1v_2+u_2v_1)+2f_{22}v_1v_2\\ 2g_{11}u_1u_2+g_{12}(u_1v_2+u_2v_1)+2g_{22}v_1v_2\end{pmatrix}+\begin{pmatrix}f_{111}u_1^3+f_{112}u_1^2v_1+f_{122}u_1v_1^2+f_{222}v_1^3\\ g_{111}u_1^3+g_{112}u_1^2v_1+g_{122}u_1v_1^2+g_{222}v_1^3\end{pmatrix},
\end{aligned} \tag{4.10}$$

and e_1,e_2,e_3 are the first-order, second-order, and third-order expansion coefficients of the control variable e respectively related to the small parameter ϵ.

Time t is also discretely defined as

$$\frac{\partial}{\partial t}=\frac{\partial}{\partial T_0}+\varepsilon\frac{\partial}{\partial T_1}+\varepsilon^2\frac{\partial}{\partial T_2}+\mathrm{O}(\varepsilon^3),\quad T_0=t,\quad T_1=\varepsilon t,\quad T_2=\varepsilon^2t.$$

Inserting the above formulas into system (4.1) and collecting the coefficients related with different orders of ϵ. The following equations are obtained that

$$O(\varepsilon):\quad L_T\begin{pmatrix}u_1\\v_1\end{pmatrix}=0, \tag{4.11a}$$

$$O(\varepsilon^2):\quad L_T\begin{pmatrix}u_2\\v_2\end{pmatrix}=\frac{\partial}{\partial T_1}\begin{pmatrix}u_1\\v_1\end{pmatrix}-e_1N\begin{pmatrix}u_1\\v_1\end{pmatrix}-n_2, \tag{4.11b}$$

$$O(\varepsilon^3):\quad L_T\begin{pmatrix}u_3\\v_3\end{pmatrix}=\frac{\partial}{\partial T_1}\begin{pmatrix}u_2\\v_2\end{pmatrix}+\frac{\partial}{\partial T_2}\begin{pmatrix}u_1\\v_1\end{pmatrix}-e_1N\begin{pmatrix}u_2\\v_2\end{pmatrix}-e_2N\begin{pmatrix}u_1\\v_1\end{pmatrix}-n_3. \tag{4.11c}$$

Part 1. Amplitude equation under first-level perturbation terms

Under the condition of first-level perturbation, let the first-level perturbation coefficients be

$$\begin{pmatrix}u_1\\v_1\end{pmatrix}=\begin{pmatrix}\varphi\\1\end{pmatrix}\left(\sum_{j=1}^{3}W_j\exp(i\mathbf{k}_j\cdot\mathbf{r})+c.c\right),\quad j=1,\ 2,\ 3, \tag{4.12}$$

where W_j represents the amplitude corresponding to mode $\exp(i\mathbf{k}_j\cdot\mathbf{r})$. Also let the zero eigenvectors of L_T^*, which is the adjoint operator subject to L_T, be

$$\mathbf{u}_j^+=\begin{pmatrix}1\\\psi\end{pmatrix}\exp(-i\mathbf{k}_j\cdot\mathbf{r})+c.c,\quad j=1,\ 2,\ 3. \tag{4.13}$$

Substituting Eq. (4.12) into the amplitude equation of $O(\varepsilon)$ order (Eq. (4.11a)), and we get the equation about φ. Similarly, ψ in Eq. (4.13) can also be solved out. Define $k_T^2 = \sqrt{\frac{\det(J)}{d_{11}d_{22}-d_{12}d_{21}}}\Big|_{e=e_T}$ as the critical wave number at e_T, and we have the following relation:

$$\varphi = -\frac{a_{12}^T - d_{12}k_T^2}{a_{11}^T - d_{11}k_T^2} = -\frac{a_{22}^T - d_{22}k_T^2}{a_{21}^T - d_{21}k_T^2}, \quad \psi = -\frac{a_{11}^T - d_{11}k_T^2}{a_{21}^T - d_{21}k_T^2} = -\frac{a_{12}^T - d_{12}k_T^2}{a_{22}^T - d_{22}k_T^2}. \tag{4.14}$$

We will only deduce the amplitude equation for W_1 only. The situation where $j = 2,\ 3$ can be obtained by simple transformation of subscript. The coefficient subject to $\exp(i\mathbf{k}_1 \cdot \mathbf{r})$ on the right side of Eq. (4.11b) is

$$\begin{pmatrix} F_x^1 \\ F_y^1 \end{pmatrix} = \frac{\partial W_1}{\partial T_1}\begin{pmatrix} \varphi \\ 1 \end{pmatrix} - e_1 N\begin{pmatrix} \varphi \\ 1 \end{pmatrix} W_1 - \begin{pmatrix} I_1 \\ I_2 \end{pmatrix} 2\overline{W}_2\overline{W}_3. \tag{4.15}$$

The Fredholm solvability condition states that if $\mathbf{u}_j^+$ and the vector on the right hand of Eq. (4.11b) are orthogonal (i.e. their dot production equals to zero), then nontrivial solution of Eq. (4.11b) exists. When $j = 1$, let $[1\ \psi]^T \cdot \left[F_x^1\ F_y^1\right]^T = 0$ and we derive the 1-order amplitude equation of system (4.1) subject to amplitude W_1.

$$(\varphi + \psi)\frac{\partial W_1}{\partial T_1} = e_1[(n_{11}\varphi + n_{12}) + \psi(n_{21}\varphi + n_{22})]W_1 + (I_1 + \psi I_2)2\overline{W}_2\overline{W}_3. \tag{4.16}$$

Part 2. Amplitude equation under second-level perturbation terms

Under the condition of second-order perturbation, we introduce higher-order perturbation terms, and express the 2-order perturbation terms as

$$\begin{aligned}\begin{pmatrix} u_2 \\ v_2 \end{pmatrix} = &\begin{pmatrix} U_0 \\ V_0 \end{pmatrix} + \sum_{j=1}^{3}\begin{pmatrix} U_j \\ V_j \end{pmatrix}\exp(i\mathbf{k}_j \cdot \mathbf{r}) + \sum_{j=1}^{3}\begin{pmatrix} U_{jj} \\ V_{jj} \end{pmatrix}\exp(2i\mathbf{k}_j \cdot \mathbf{r}) \\ &+\begin{pmatrix} U_{12} \\ V_{12} \end{pmatrix}\exp(i(\mathbf{k}_1 - \mathbf{k}_2) \cdot \mathbf{r}) + \begin{pmatrix} U_{23} \\ V_{23} \end{pmatrix}\exp(i(\mathbf{k}_2 - \mathbf{k}_3) \cdot \mathbf{r}) + \begin{pmatrix} U_{31} \\ V_{31} \end{pmatrix}\exp(i(\mathbf{k}_3 - \mathbf{k}_1) \cdot \mathbf{r}) + c.c.\end{aligned} \tag{4.17}$$

Substitute it into Eq. (4.11b), and let coefficients of different orders of e (natural logarithm) on both sides of the equation be equal. The expression of the perturbation terms can be obtained as follows.

1. Coefficients of $\exp(0)$.

$$left = L_T\begin{pmatrix} U_0 \\ V_0 \end{pmatrix} = -2\begin{pmatrix} I_1 \\ I_2 \end{pmatrix}\left(|W_1|^2 + |W_2|^2 + |W_3|^2\right) = right, \tag{4.18}$$

multiplying the inverse matrix of L_T on both sides of the equation, and we have

$$\begin{pmatrix} U_0 \\ V_0 \end{pmatrix} = \frac{-2\left(|W_1|^2 + |W_2|^2 + |W_3|^2\right)}{a_{11}^T a_{22}^T - a_{12}^T a_{22}^T}\begin{pmatrix} a_{22}^T & -a_{12}^T \\ -a_{21}^T & a_{11}^T \end{pmatrix}\begin{pmatrix} I_1 \\ I_2 \end{pmatrix} = \left(|W_1|^2 + |W_2|^2 + |W_3|^2\right)\begin{pmatrix} u_{00} \\ v_{00} \end{pmatrix}. \tag{4.19}$$

2. Coefficients of $\exp(i\mathbf{k}_j \cdot \mathbf{r})$. Here we will deduce the amplitude equation for $j = 1$ only. The situation where $j = 2$and 3 can be obtained by simple transformation of subscript. Since the right side of the equation contains other variables, we cannot find the exact expression of U_1 and V_1, but we can find a relationship between them. Let $U_1 = f \cdot V_1$, and we have

$$left = \left(L_T - k_T^2 D\right)\begin{pmatrix} fV_1 \\ V_1 \end{pmatrix} = \begin{pmatrix} F_x^1 \\ F_y^1 \end{pmatrix} = right. \tag{4.20}$$

Solving Eq. (4.20) gives that

$$\begin{aligned} f &= \frac{-\left(a_{22}^T - d_{22}k_T^2\right)F_y^1 + \left(a_{12}^T - d_{12}k_T^2\right)F_x^1}{\left(a_{21}^T - d_{21}k_T^2\right)F_y^1 - \left(a_{11}^T - d_{11}k_T^2\right)F_x^1} \\ &= \frac{\left(-\frac{a_{22}^T - d_{22}k_T^2}{a_{21}^T - d_{21}k_T^2}\right)\cdot\frac{F_y^1}{a_{11}^T - d_{11}k_T^2} + \left(-\frac{a_{12}^T - d_{12}k_T^2}{a_{11}^T - d_{11}k_T^2}\right)\cdot\left(-\frac{F_x^1}{a_{21}^T - d_{21}k_T^2}\right)}{\frac{F_y^1}{a_{11}^T - d_{11}k_T^2} - \frac{F_x^1}{a_{21}^T - d_{21}k_T^2}} = \varphi. \end{aligned} \tag{4.21}$$

Applying similar process to situations where $j = 2$ and 3, it is found the following relationship exists that $U_j = \varphi \cdot V_j\ (j = 1, 2, 3)$.

3. Coefficients of $\exp(2i\mathbf{k}_j \cdot \mathbf{r})$. When $j = 1$,

$$left = \left(L_T - 4k_T^2 D\right)\begin{pmatrix} U_{11} \\ V_{11} \end{pmatrix} = -\begin{pmatrix} I_1 \\ I_2 \end{pmatrix} W_1^2 = right, \tag{4.22}$$

multiplying the inverse matrix of $L_T - 4k_T^2 D$ on both sides of the equation, and we obtain

$$\begin{aligned} \begin{pmatrix} U_{11} \\ V_{11} \end{pmatrix} &= \frac{-{W_1}^2}{\mathrm{Det}_{11}} \begin{pmatrix} a_{22}^T - 4d_{22}k_T^2 & -\left(a_{12}^T - 4d_{12}k_T^2\right) \\ -\left(a_{21}^T - 4d_{21}k_T^2\right) & a_{11}^T - 4d_{11}k_T^2 \end{pmatrix} \begin{pmatrix} I_1 \\ I_2 \end{pmatrix} = W_1^2 \begin{pmatrix} u_{11} \\ v_{11} \end{pmatrix}, \\ \mathrm{Det}_{11} &= \left(a_{11}^T - 4d_{11}k_T^2\right)\left(a_{22}^T - 4d_{22}k_T^2\right) - \left(a_{12}^T - 4d_{12}k_T^2\right)\left(a_{21}^T - 4d_{21}k_T^2\right). \end{aligned} \tag{4.23}$$

Applying similar process to situations where $j = 2$ and 3, it is found the following relationship exists that

$$\begin{pmatrix} U_{jj} \\ V_{jj} \end{pmatrix} = W_j^2 \begin{pmatrix} u_{11} \\ v_{11} \end{pmatrix}, \quad j = 1, 2, 3. \tag{4.24}$$

4. Coefficients of $\exp\left(i(\mathbf{k}_1 - \mathbf{k}_2)\cdot\mathbf{r}\right)$. The following relationship exists

$$\begin{aligned} \Delta[\exp\left(i(\mathbf{k}_1 - \mathbf{k}_2)\cdot\mathbf{r}\right)] &= -(\mathbf{k}_1 - \mathbf{k}_2)^2 \cdot \exp\left(i(\mathbf{k}_1 - \mathbf{k}_2)\cdot\mathbf{r}\right) \\ &= -\left(\mathbf{k}_1^2 + \mathbf{k}_2^2 - 2|\mathbf{k}_1||\mathbf{k}_2|\cos\left(\tfrac{2\pi}{3}\right)\right)\cdot \exp\left(i(\mathbf{k}_1 - \mathbf{k}_2)\cdot\mathbf{r}\right) \\ &= -3k_T^2 \cdot \exp\left(i(\mathbf{k}_1 - \mathbf{k}_2)\cdot\mathbf{r}\right). \end{aligned} \tag{4.25}$$

Collect the coefficients of $\exp\left(i(\mathbf{k}_1 - \mathbf{k}_2)\cdot\mathbf{r}\right)$ in Eq. (4.11b) and we have

$$left = \left(L_T - 3k_T^2 D\right)\begin{pmatrix} U_{12} \\ V_{12} \end{pmatrix} = -2W_1\bar{W}_2 \begin{pmatrix} I_1 \\ I_2 \end{pmatrix} = right. \tag{4.26}$$

Thus

$$\begin{aligned} \begin{pmatrix} U_{12} \\ V_{12} \end{pmatrix} &= \frac{-2W_1\bar{W}_2}{\mathrm{Det}_{22}} \begin{pmatrix} a_{22}^T - 3d_{22}k_T^2 & -\left(a_{12}^T - 3d_{12}k_T^2\right) \\ -\left(a_{21}^T - 3d_{21}k_T^2\right) & a_{11}^T - 3d_{11}k_T^2 \end{pmatrix} \begin{pmatrix} I_1 \\ I_2 \end{pmatrix} = W_1\bar{W}_2 \begin{pmatrix} u_{22} \\ v_{22} \end{pmatrix}, \\ \mathrm{Det}_{22} &= \left(a_{11}^T - 3d_{11}k_T^2\right)\left(a_{22}^T - 3d_{22}k_T^2\right) - \left(a_{12}^T - 3d_{12}k_T^2\right)\left(a_{21}^T - 3d_{21}k_T^2\right). \end{aligned} \tag{4.27}$$

The remaining coefficients can be obtained by subscript transformation:

$$\begin{pmatrix} U_{kl} \\ V_{kl} \end{pmatrix} = \begin{pmatrix} u_{22} \\ v_{22} \end{pmatrix} W_k \bar{W}_l, \quad k,\ l = 1, 2, 3,\ k \neq l. \tag{4.28}$$

After obtaining the expression for coefficients of high-order perturbation terms in Eq. (4.17), consider $\left[G_x^1\ G_y^1\right]$, the coefficients of $\exp\left(i\mathbf{k}_1\mathbf{r}\right)$ on the right side of Eq. (4.11c). It is the $O(\varepsilon^3)$ order expansion of the system near the critical value of controlling variable e_T.

$$\begin{pmatrix} G_x^1 \\ G_y^1 \end{pmatrix} = \left(\frac{\partial V_1}{\partial T_1} + \frac{\partial W_1}{\partial T_2}\right)\begin{pmatrix} \varphi \\ 1 \end{pmatrix} - (e_1 V_1 + e_2 W_1) N \begin{pmatrix} \varphi \\ 1 \end{pmatrix} - G_{n_3}, \tag{4.29}$$

where G_{n_3} represents the coefficients of $\exp\left(i\mathbf{k}_1\mathbf{r}\right)$ contributed by n_3, which has been expressed already in Eq. (4.10). n_3 is divided into two parts: the second-order nonlinear expansion terms and the third-order nonlinear expansion terms. Below we will analyze the coefficients contributed by them separately.

Second-order expansion items in n_3 each provides:

- $u_1 u_2 : \varphi^2 \cdot (\bar{W}_2\bar{V}_3 + \bar{W}_3\bar{V}_2) + \varphi \cdot \left((u_{00} + u_{11})|W_1|^2 + (u_{00} + u_{22}) \cdot \left(|W_2|^2 + |W_3|^2\right)\right) \cdot W_1,$
- $u_1 v_2 : \varphi \cdot (\bar{W}_2\bar{V}_3 + \bar{W}_3\bar{V}_2) + \varphi \cdot \left((v_{00} + v_{11})|W_1|^2 + (v_{00} + v_{22}) \cdot \left(|W_2|^2 + |W_3|^2\right)\right) \cdot W_1,$
- $u_2 v_1 : \varphi \cdot (\bar{W}_2\bar{V}_3 + \bar{W}_3\bar{V}_2) + \varphi \cdot \left((u_{00} + u_{11})|W_1|^2 + (u_{00} + u_{22}) \cdot \left(|W_2|^2 + |W_3|^2\right)\right) \cdot W_1,$
- $v_1 v_2 : (\bar{W}_2\bar{V}_3 + \bar{W}_3\bar{V}_2) + \varphi \cdot \left((v_{00} + v_{11})|W_1|^2 + (v_{00} + v_{22}) \cdot \left(|W_2|^2 + |W_3|^2\right)\right) \cdot W_1.$

Third-order expansion items in n_3 each provides:

- $u_1^3 : \varphi^3 \cdot \left(3|W_1|^2 + 6|W_2|^2 + 6|W_3|^2\right) W_1,$

- $u_1^2 v_1 : \varphi^2 \cdot \left(3|W_1|^2 + 6|W_2|^2 + 6|W_3|^2\right) W_1$,
- $u_1 v_1^2 : \varphi \cdot \left(3|W_1|^2 + 6|W_2|^2 + 6|W_3|^2\right) W_1$,
- $v_1^3 : \left(3|W_1|^2 + 6|W_2|^2 + 6|W_3|^2\right) W_1$.

As a result, we obtain the coefficients of $\exp(-i\mathbf{k}_1\mathbf{r})$ contributed by n_3:

$$\begin{aligned} G_{n_3} = \; & 2\begin{pmatrix} I_1 \\ I_2 \end{pmatrix}(\bar{W}_2\bar{V}_3 + \bar{W}_3\bar{V}_2) + \begin{pmatrix} H_1 & H_3 \\ H_2 & H_4 \end{pmatrix}\begin{pmatrix} |W_1|^2(u_{00}+u_{11}) + \left(|W_2|^2 + |W_3|^2\right)(u_{00}+u_{22}) \\ |W_1|^2(v_{00}+v_{11}) + \left(|W_2|^2 + |W_3|^2\right)(v_{00}+v_{22}) \end{pmatrix} \\ & + \begin{pmatrix} R_1 \\ R_2 \end{pmatrix}\left(3|W_1|^2 + 6|W_2|^2 + 6|W_3|^2\right). \end{aligned} \tag{4.30}$$

Using Fredholm's solvability condition $[1 \;\; \psi]^T \cdot \left[G_x^1 \;\; G_y^1\right]^T = 0$, and we obtain

$$\begin{aligned} (\varphi+\psi)\left(\tfrac{\partial V_1}{\partial T_1} + \tfrac{\partial W_1}{\partial T_2}\right) \; & = [(\varphi n_{11} + n_{12}) + \psi(\varphi n_{21} + n_{22})](e_1 V_1 + e_2 W_1) \\ & \quad + 2(I_1 + \psi I_2)(\overline{W}_2\overline{V}_3 + \overline{W}_3\overline{V}_2) - \left[G_1|W_1|^2 + G_2\left(|W_2|^2 + |W_3|^2\right)\right] W_1. \end{aligned} \tag{4.31}$$

Below we use the relationship

$$A_j = \varepsilon W_j + \varepsilon^2 V_j + \mathrm{O}(\varepsilon^3) \tag{4.32}$$

and the amplitude equation under the first-order perturbation (Eq. (4.16)))) to derive the expression of the amplitude equation under the second-order perturbation. We assume that the amplitude A_j $(j = 1, 2, 3)$ changes with time slowly such that $\frac{\partial A_j}{\partial T_0} = 0$. So A_j is only affected by higher order time scales:

$$\frac{\partial A_j}{\partial t} = \left(\varepsilon\frac{\partial}{\partial T_1} + \varepsilon^2\frac{\partial}{\partial T_2} + \cdots\right)\cdot\left(\varepsilon W_j + \varepsilon^2 V_j + \cdots\right) = \varepsilon^2\frac{\partial W_j}{\partial T_1} + \varepsilon^3\cdot\left(\frac{\partial W_j}{\partial T_2} + \frac{\partial V_j}{\partial T_1}\right) + \cdots. \tag{4.33}$$

We can also expand the following terms into:

$$\begin{aligned} & (e_T - e)\cdot A_j = (\varepsilon e_1 + \varepsilon^2 e_2 + \cdots)\cdot(\varepsilon W_j + \varepsilon^2 V_j + \cdots) = \varepsilon^2(e_1 W_j) + \varepsilon^3\cdot(e_2 W_j + e_1 V_j) + \cdots, \\ & \bar{A}_2\bar{A}_3 = (\varepsilon\bar{W}_2 + \varepsilon^2\bar{V}_2 + \cdots)\cdot(\varepsilon\bar{W}_3 + \varepsilon^2\bar{V}_3 + \cdots) = \varepsilon^2\bar{W}_2\bar{W}_3 + \varepsilon^3\cdot(\bar{W}_3\bar{V}_2 + \bar{W}_2\bar{V}_3) + \cdots, \\ & |A_1|^2 A_1 = (\varepsilon W_2 + \varepsilon^2 V_2)\cdot(\varepsilon\bar{W}_1 + \varepsilon^2\bar{V}_1)\cdot(\varepsilon W_1 + \varepsilon^2 V_1) = \varepsilon^3|W_1|^2 W_1 + \cdots, \\ & |A_2|^2 A_1 = (\varepsilon W_2 + \varepsilon^2 V_2)\cdot(\varepsilon\bar{W}_2 + \varepsilon^2\bar{V}_2)\cdot(\varepsilon W_1 + \varepsilon^2 V_1) = \varepsilon^3|W_2|^2 W_1 + \cdots, \\ & |A_3|^2 A_1 = (\varepsilon W_3 + \varepsilon^2 V_3)\cdot(\varepsilon\bar{W}_3 + \varepsilon^2\bar{V}_3)\cdot(\varepsilon W_1 + \varepsilon^2 V_1) = \varepsilon^3|W_3|^2 W_1 + \cdots. \end{aligned} \tag{4.34}$$

Substitute the above items into $\varepsilon^2\cdot$ (4.16) $+\varepsilon^3\cdot$ (4.31). By rearranging the terms, we arrive at the final amplitude equation under second-order perturbations, which is described in Eq. (4.7).

4.2. Stability analysis of the amplitude equation

The conditions for the appearance of stable Turing patterns can be obtained by analyzing the stable solutions of Eq. (4.7). The theoretical derivation in this regard is very complete and has been done by many researchers. For example, Qi. Quyang gave a very detailed derivation process in his book [26] in 2010. In this part, we also refers to the work of Yuan et al. [20], Kuramoto et al. [15] and Cruywagen et al. [8].

Theorem 4.2. *Set $\phi = \phi_1 + \phi_2 + \phi_3, \rho_j = |A_j|, A_j = \rho_j e^{i\phi_i}$. Amplitude equation under second-order perturbations, Eq. (4.7), can be changed to the following equation after substitution:*

$$\begin{cases} \tau_0\frac{\partial\phi}{\partial t} = -h\frac{\rho_1^2\rho_2^2 + \rho_1^2\rho_3^2 + \rho_2^2\rho_3^2}{\rho_1\rho_2\rho_3}\sin\phi, \\ \tau_0\frac{\partial\rho_1}{\partial t} = \eta\rho_1 + h\rho_2\rho_3\cos\phi - g_1\rho_1^3 - g_2(\rho_2^2 + \rho_3^2)\rho_1, \\ \tau_0\frac{\partial\rho_2}{\partial t} = \eta\rho_2 + h\rho_1\rho_3\cos\phi - g_1\rho_2^3 - g_2(\rho_1^2 + \rho_3^2)\rho_2, \\ \tau_0\frac{\partial\rho_3}{\partial t} = \eta\rho_3 + h\rho_2\rho_1\cos\phi - g_1\rho_3^3 - g_2(\rho_1^2 + \rho_2^2)\rho_3. \end{cases} \tag{4.35}$$

We define four critical values of η here:

$$\eta_1 = -\frac{h^2}{4(g_1+2g_2)}, \quad \eta_2 = 0, \quad \eta_3 = \frac{h^2 g_1}{(g_2-g_1)^2}, \quad \eta_4 = \frac{h^2(2g_1+g_2)}{(g_2-g_1)^2}. \tag{4.36}$$

There are four kinds of stable solutions to this equation.

1. *Homogeneous stationary solution:*

   $$\rho_1 = \rho_2 = \rho_3 = 0,$$

   with stable condition $\eta < \eta_2 = 0$.
2. *Striped pattern solution:*

   $$\rho_1 = \sqrt{\frac{\mu}{g_1}} \neq 0, \quad \rho_2 = \rho_3 = 0,$$

   with stable condition $\eta > \eta_3$.
3. *Hexagonal pattern solution:*

   $$\rho_1 = \rho_2 = \rho_3 = \frac{|h| \pm \sqrt{h^2 + 4(g_1+2g_2)\eta}}{2(g_1+2g_2)},$$

   with stable condition $\eta > \eta_1$. *Denote*

   $$\rho^+ = \frac{|h| + \sqrt{h^2 + 4(g_1+2g_2)\eta}}{2(g_1+2g_2)}, \quad \rho^- = \frac{|h| - \sqrt{h^2 + 4(g_1+2g_2)\eta}}{2(g_1+2g_2)},$$

   ρ^+ *is stable if* $\eta < \eta_4$ *and* ρ^- *is always unstable.*
4. Mixed pattern solution:

   $$\rho_1 = \frac{|h|}{g_2-g_1}, \quad \rho_2 = \rho_3 = \sqrt{\frac{\eta - g_1\rho_1^2}{g_1+g_2}},$$

   with the existence condition $g_2 > g_1,\ \eta > g_1\rho_1^2$ *and is always unstable.*

Proof. After obtaining Eq. (4.35), the methods for analyzing the stability of solutions of the four types of amplitude equations have been analyzed exhaustively in many books and papers, so the process will not be repeated here. Here we will simply describe the process of deriving Eq. (4.35) from the amplitude equation under the second-level perturbation.

After setting $\phi = \phi_1 + \phi_2 + \phi_3, \rho_j = |A_j|, A_j = \rho_j e^{i\phi_i}$, we have the following relationships:

$$\frac{\partial A_j}{\partial t} = e^{i\phi_i}\left(\rho_i \frac{\partial \phi_i}{\partial t} i + \frac{\partial \rho_i}{\partial t}\right), \quad e^{-\phi i} = \cos\phi - i\sin\phi.$$

Insert them into Eq. (4.7). By separating the real and imaginary parts, we have

$$\begin{cases} \tau_0 \frac{\partial \phi_1}{\partial t} = -h\frac{\rho_2\rho_3}{\rho_1}\sin\phi, \\ \tau_0 \frac{\partial \rho_1}{\partial t} = \eta\rho_1 + h\rho_2\rho_3\cos\phi - g_1\rho_1^3 - g_2(\rho_2^2+\rho_3^2)\rho_1, \end{cases} \tag{4.37}$$

for $j = 1$. Apply similar process to $j = 2$ and 3, we obtain Eq. (4.35).

Remark 4.1. In second-order amplitude equation Eq. (4.7), the coefficient of the second-order terms h must be small enough, or at most on the same order of magnitude as the third-order terms' coefficients. In addition, since $|h|$ is always positive, it is also one of the trigger factors for the instability of system. In order for the existence of stable solutions in the system, the third-order terms' coefficients g_1 and g_2 must be positive. Otherwise higher order perturbations must be included to explain the shapes of patterns.

Remark 4.2. It is easy to see that when $h^2 \neq 0$, the relationship between the critical points is $\eta_1 < \eta_2 = 0 < \eta_3 < \eta_4$. From the above analysis of the shape of the amplitude equation, it can be also seen that when $\eta_2 < \eta < \eta_3$, hexagonal patterns will occur in the system. There are two types of hexagonal patterns. If the second-order coefficient $h > 0$, then hexagon pattern is H_0; otherwise, it is H_π. When $\eta_3 < \eta < \eta_4$, the system has a bistable state where the hexagon patterns and the striped patterns coexist. $\eta > \eta_4$, the system transitions from hexagon patterns to striped patterns.

4.3. Derivation of amplitude equation for system (1) ($\tau = 0$)

Since the deduction of amplitude equation in the precious subsection is proceeded under system with no time delay, we consider $\tau = 0$ in system (1) in the following. In this condition, just let $\tau = 0$ in the conditions (C1)-(C3), and we arrive at the

conditions for the emergence Turing bifurcation in the non-delayed system. It can be verified that after removing the time delay term, the emergence condition of diffusion-induced Turing bifurcation remains the same as the original system. This is due to our previous assumption that τ is very small such that $m_{11} > 0$.

In the non-delayed new system, one can calculate that

$$\begin{aligned}
&f_{11} = \left(1 - \tfrac{r\mu}{K\beta}\right)\left(\tfrac{1}{K} + \tfrac{1}{A}\right) - \tfrac{\mu r}{AK\beta}, \quad f_{12} = -2\sqrt{-\tfrac{r\left(\mu^2 - \beta\mu(A+K) + AK\beta^2\right)}{AK\beta}}, \quad f_{22} = -\mu,\\
&g_{11} = 0, \quad g_{12} = 2\sqrt{-\tfrac{r\left(\mu^2 - \beta\mu(A+K) + AK\beta^2\right)}{AK\beta}}, \quad g_{22} = 0,\\
&f_{111} = -\tfrac{r}{AK}, \quad f_{112} = 0, \quad f_{122} = -\beta, \quad f_{222} = 0,\\
&g_{111} = 0, \quad g_{112} = 0, \quad g_{122} = \beta, \quad g_{222} = 0.
\end{aligned} \tag{4.38}$$

Next, using the conclusions of the previous subsection, we can calculate the amplitude equation for this system. Since the derivation of the amplitude equation mentioned above is carried out near μ_{t_2}, which is the critical value of the control variable μ. The value of μ_{t_2} is substituted in μ in the calculation as for approximation.

In order to better present the analysis results, we plot Fig. 2, which illustrates how mode ρ changes with η. The values of parameters are consistent with those in Fig. 1 except for $\tau = 0$. From the theory of the amplitude equation, we calculate: $h = 0.1284,\ g_1 = 15.7571,\ g_2 = 17.4495$. Therefore, the hexagonal pattern in the system is H_0 since $h < 0$. The critical values η are $\eta_1,\ \eta_2,\ \eta_3,\ \eta_4 = -0.00008142,\ 0,\ 0.09076.\ 0.2820$. The corresponding critical values of control parameters μ can be calculated via $\mu_i = \mu_{t_2}(1 - \eta_i) : \mu_1,\ \mu_2,\ \mu_3,\ \mu_4 = 0.7925,\ 0.7924,\ 0.7205,\ 0.5689$.

5. Numerical simulation

In this part, we first use numerical algorithms to simulate the non-delayed system based on the amplitude equation theorem derived above. The simulation results are consistent with the amplitude equation. When the time delay is added and other conditions remain unchanged, we also explore its effect on the shape of the patterns via comparison. Finally, this article selects three network structures: "LA4", "LA12", and "WS", the change of the density of susceptible group (S) over time is studied while other conditions remain the same.

Our numerical method is based on "Forward Euler Method". Time and space are discretized into small steps $\Delta t = 0.01, \Delta x = 1$ separately. The two-dimensional simulation region is $\Omega = [0, 100] \times [0, 100]$ under Neumann boundary condition.

Initial conditions are chosen around the rumor-spreading equilibrium point E^*, and the perturbation terms are given by

$$\begin{aligned}
S(0, x, y) &= S^* \cdot (1 + 0.0005 * \mathrm{randn}(0, 1)),\\
I(0, x, y) &= I^* \cdot (1 + 0.0005 * \mathrm{randn}(0, 1)).
\end{aligned} \tag{4.39}$$

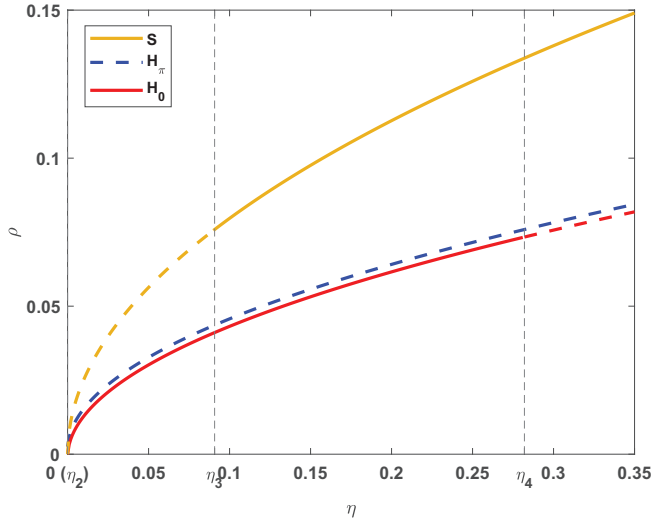

Fig. 2. Bifurcation diagram of amplitude equations' solutions. The solid line indicates that the solution is stable, and the dotted line is unstable. S represents the striped pattern. H_0 represents the patterns of $\phi = 0$, and H_π represents the patterns of $\phi = \pi$. Control parameter $\mu = \mu_{t_2} = 0.7924$, and the values of other variables are fixed as: $r = 0.1,\ K = 1,\ A = 0.3,\ \beta = 0.8,\ d_{11} = 5.5,\ d_{12} = 0.7,\ d_{21} = 0.8,\ d_{22} = 0.2$.

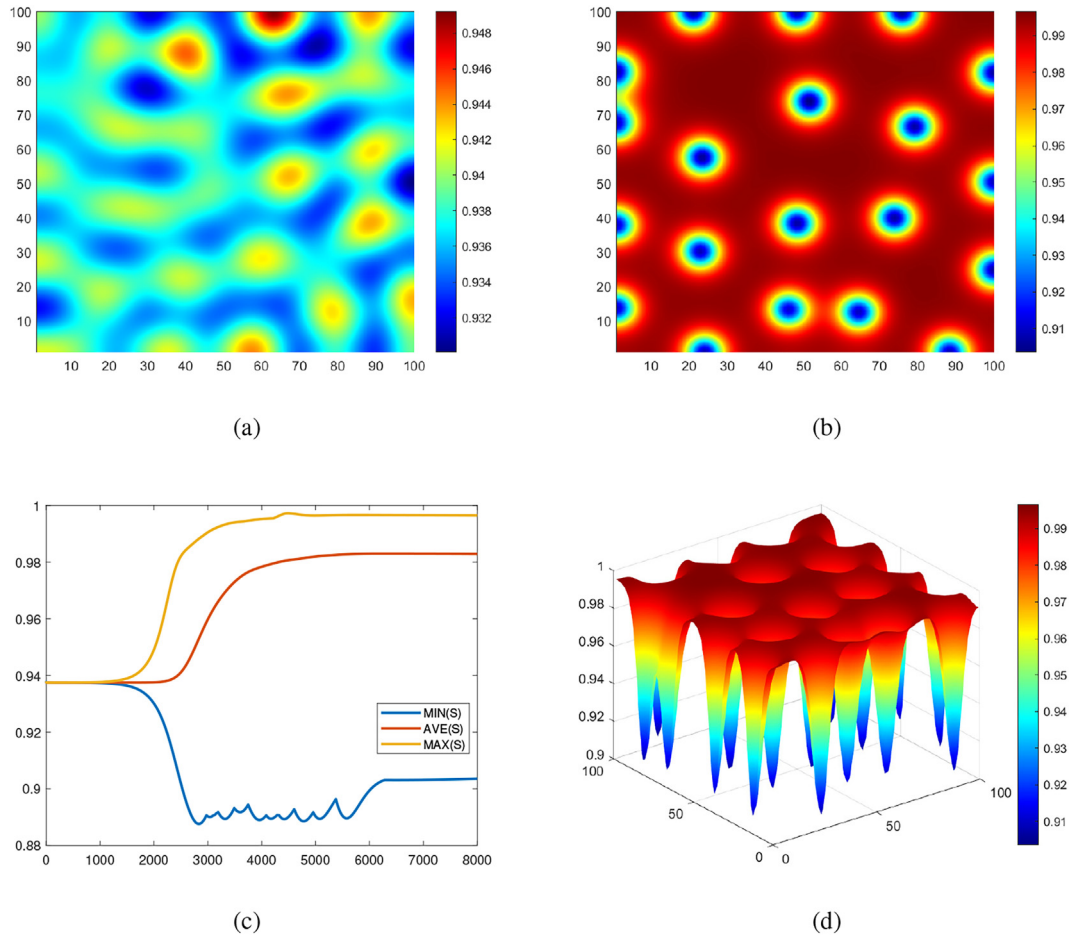

Fig. 3. The pattern when the control variable $\mu = 0.75$. The time is: Fig. 3a, $t = 2000$; Fig. 3b, $t = 8000$. Fig. 3c: the maximum, average, minimum value of S (susceptible) with time increasing from $t = 0$ to $t = 8000$. Fig. 3d: the three-dimensional sketch pattern at $t = 8000$.

The random small perturbations are generated by "randn" function in Matlab: The random seeds are set using "rng" function to ensure other conditions are the same.

5.1. Pattern formation in the non-delayed system

We fix the values of variables at: $r = 0.1,\ K = 1,\ A = 0.3,\ \beta = 0.8,\ d_{11} = 5.5,\ d_{12} = 0.7,\ d_{21} = 0.8,\ d_{22} = 0.2$. The critical value of the control variable $\mu = \mu_{t_2} = 0.7924$. According to Eq. (3.16), the conditions for the occurrence of Turing bifurcation require $0.52 < \mu < 0.7924$. From the calculation in the previous section, four critical values of μ are $\mu_1,\ \mu_2,\ \mu_3,\ \mu_4 = 0.7925,\ 0.7924,\ 0.7205,\ 0.5689$, and three of them are feasible. Thus three types of patterns can be observed in our system.

Let $\mu = 0.75$, and $\eta \in (\eta_2,\ \eta_3)$. The system should present H_0 hexagonal pattern according to our theorem. When $t = 2000$, the density of susceptible individuals across the space begin to diverge, especially in the right half of Fig. 3a. When $t = 3000 \sim 6000$, the minimum value for the density of susceptible individuals begins to fluctuate up and down. After $t = 6000$ there is a significant increase, and then it stabilizes. When $t = 8000$, the system presents stable hexagonal pattern H_0, which is reflected as low-density blue pits on the three-dimensional picture. At this time, the rumor spreaders are only confined to the blue spotted low-density areas. Susceptible individuals (S) have a higher density throughout the whole area.

Let $\mu = 0.65$, and $\eta \in (\eta_3,\ \eta_4)$. The system should present the bistable state of the striped patterns and the H_0 hexagonal patterns. When $t = 2000$, there is competition between the hexagonal patterns and the striped patterns. After $t = 3000$, the density of susceptible individuals begins to stabilize. When $t = 10000$, the competition ends, forming a bistable state where the hexagonal patterns H_0 and the striped patterns coexist. The hexagonal patterns are mainly concentrated in the upper and middle part of Fig. 4a, while the striped patterns appear in the lower left and upper right corners of the panel. Rumors spread more widely compared with spot patterns.

Let $\mu = 0.55$, and $\eta > \eta_4$. The hexagonal patterns are unstable, and only the striped patterns can be observed in the system. When $t = 4000$, there is competition between the hexagonal patterns and the striped patterns. Minor fluctuations occur in the maximum and minimum values of the density for susceptible individuals. When $t = 10000$, the system displays striped patterns as shown in Fig. 5. Rumors prevail in the blue striped areas. The areas of regions where rumors are prevalent are almost the same as the area of non-prevalent ones.

5.2. Pattern formation in the delayed system

In this part, we fix the values of other variables the same as the section above, and add time delay into the system to explore its effect on the shapes of the patterns. According to Theorem 3.3, $m_{11} = 1 - \tau \frac{rS^*}{K} \cdot \left(\frac{S^*}{A} - 1\right) > 0$, it can be concluded that if the condition $\tau < 7.2046$ holds, the appearance condition of Turing bifurcation remains the same as Eq. (3.16).

We choose the same variable values and initial conditions as Fig. 4, and set $\tau = 1$ in our simulations. When $t = 4000$, the patterns are basically formed, with more striped patterns than hexagonal ones. When $t = 10000$, the striped pattern in the middle of the panel is splitted into two small hexagonal patterns. It is worth mentioning that the striped pattern on the top still retains its strip shape other than splitting into spotted ones as shown in Fig. 6. It is different from Fig. 4. In addition, when $t = 2000 \sim 4000$, the minimum value for the density of susceptible individuals experiences some minor fluctuations, which are not seen in the model with no time delay. From the above results, it can be inferred that the time delay term will slow down the process of the striped patterns breaking into hexagonal patterns. Those are the effects of time delay on the system.

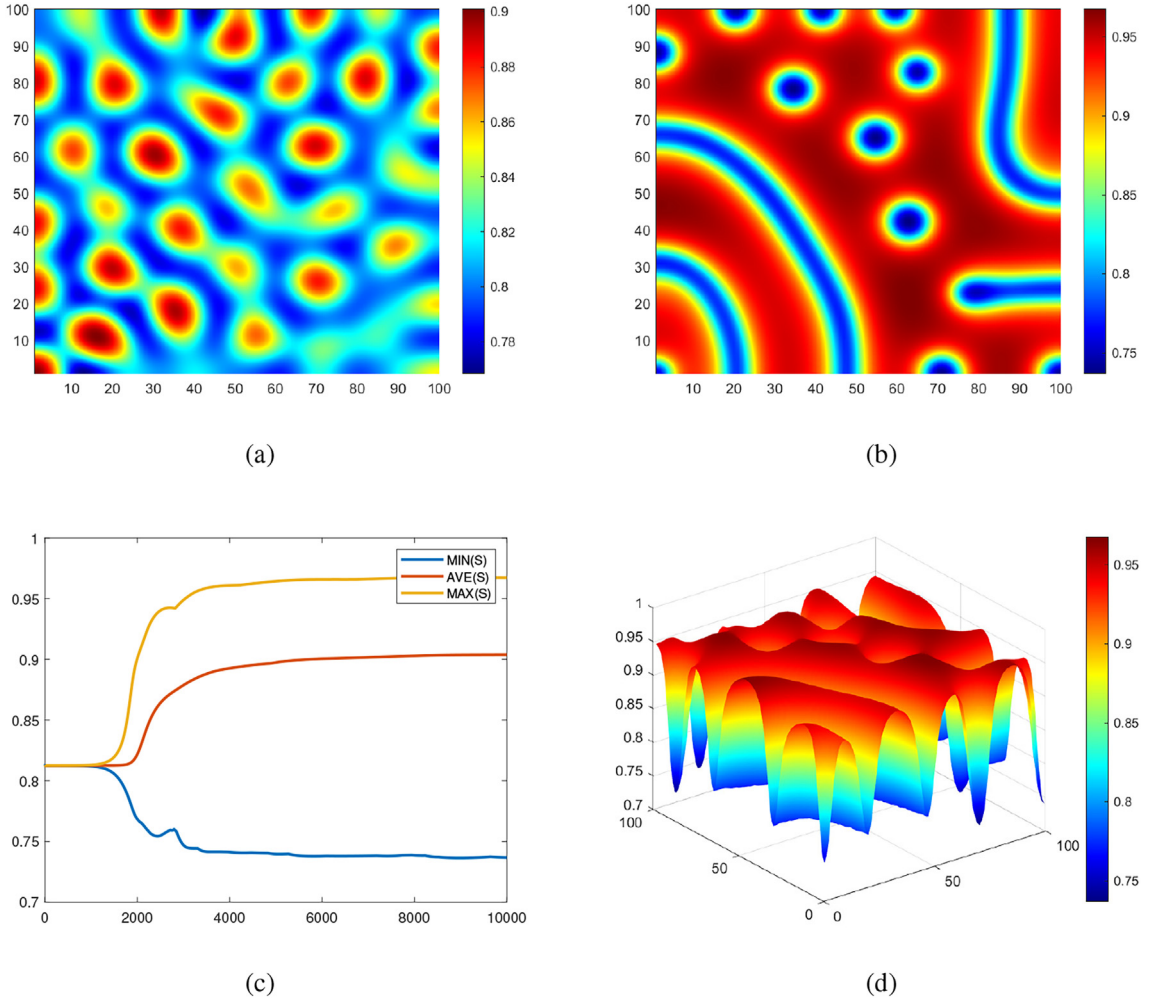

Fig. 4. The pattern when the control variable $\mu = 0.65$. The time is: Fig. 4a, $t = 2000$; Fig. 4b, $t = 10000$. Fig. 4c: the maximum, average, minimum value of S (susceptible) with time increasing from $t = 0$ to $t = 10000$. Fig. 4d: the three-dimensional sketch pattern at $t = 10000$.

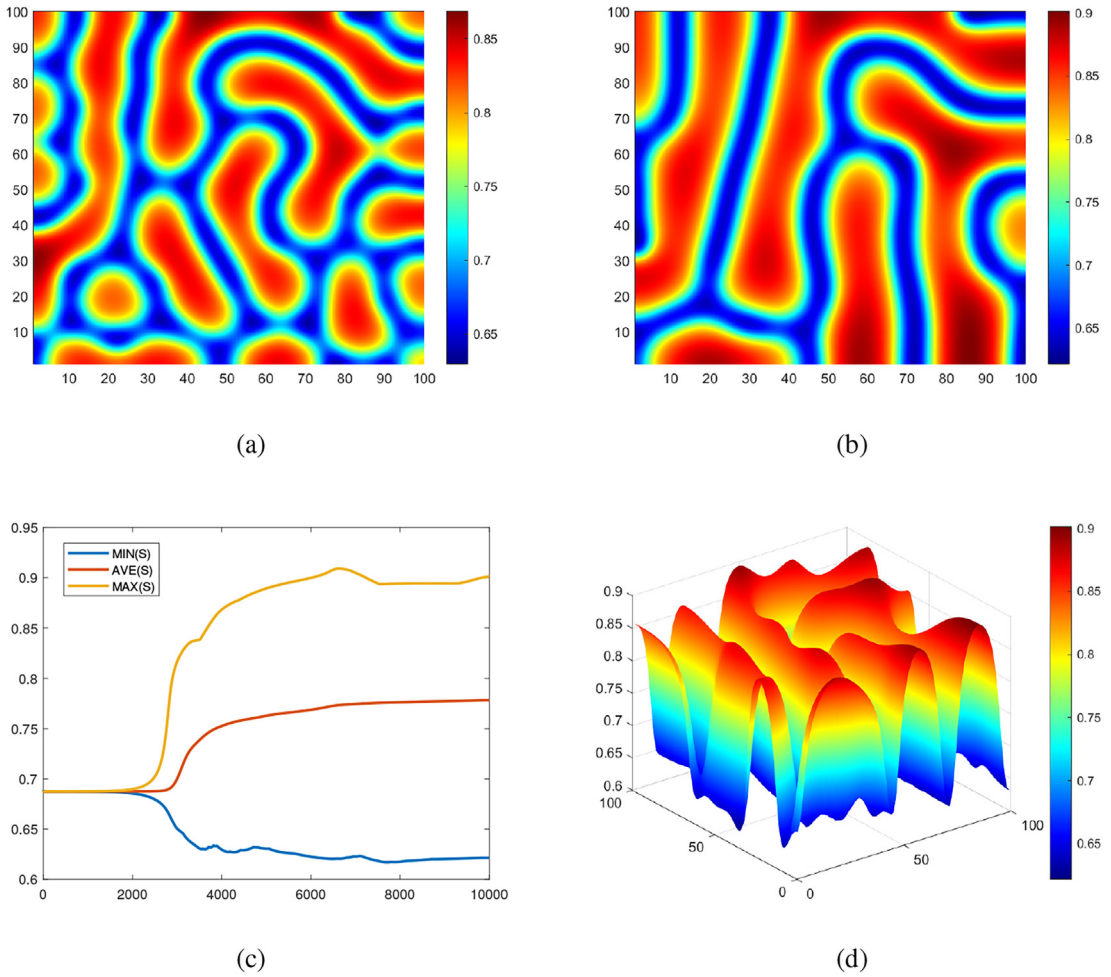

Fig. 5. The pattern when the control variable $\mu = 0.55$. The time is: Fig. 5a, $t = 4000$; Fig. 5b, $t = 10000$. Fig. 5c: the maximum, average, minimum value of S (susceptible) with time increasing from $t = 0$ to $t = 10000$. Fig. 5d: the three-dimensional sketch pattern at $t = 10000$.

5.3. Pattern formation under networks structures

On LA networks, nodes are arranged in a square lattices. In the "LA4" network, each node is connected to its 4 adjacent nodes. In the "LA12" network, each node is connected to its 12 adjacent nodes. Their average degree $\langle k \rangle$ = 4 and 12. The WS (Watts-Strogatz) small-world random networks are networks between regular networks and random networks. Therefore, the model starts from a completely regular network and disrupts and reconnects the edges in the network with a certain probability.

The blue line around 0.8125 in the first three figures Fig. 7 represents the density of susceptible individuals of each node in the initial state. In the "LA4" and "LA12" networks, there are certain nodes whose upper and lower bounds of the density of susceptible individuals are smaller. In the "WS" small world networks, the density of susceptible individuals of nodes is more divergent, mainly concentrated in the vicinity of $0.9 \sim 0.95$ or below 0.8. The distribution of nodes in other parts is relatively sparse.

In every simulation, we draw the density distributions of 900 nodes on one panel at different time before $t = 5000$. The horizontal axes of Fig. 7a, 7b, 7c represents the index of nodes and the vertical axes of them represents the density of susceptible individuals.

By comparing the last three figures, it can be seen that the network structure can affect the time when the maximum, minimum, and average values of the density of susceptible individuals at each node begin to diverge. In the "LA4" network, the three lines diverged about 500 time steps earlier than the "LA12" network. In the "WS" network, this time is further advanced, and there are more fluctuations as the three lines stabilize.

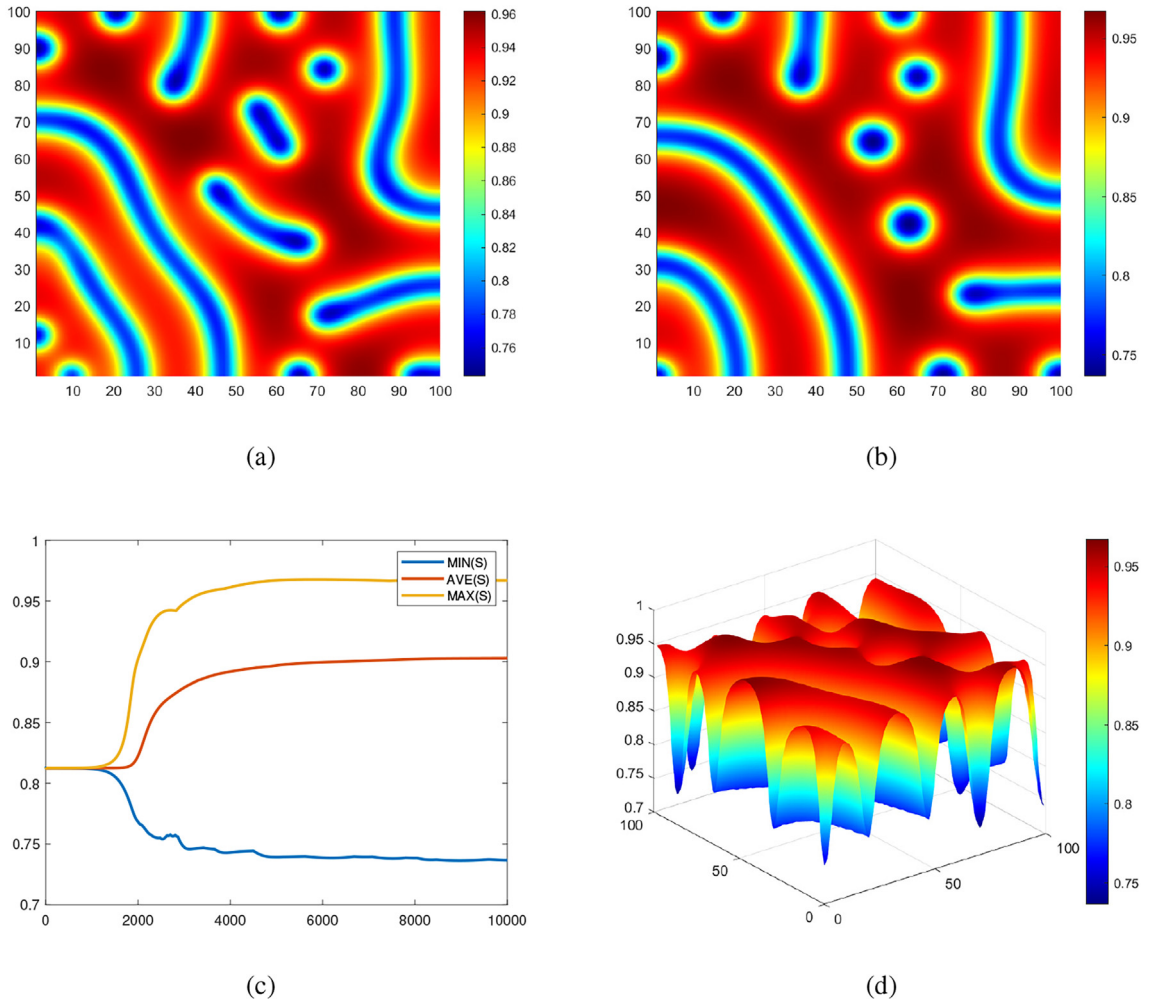

Fig. 6. The pattern when the control variable $\mu = 0.65$ and time delay $\tau = 1$. The time is: Fig. 6a, $t = 4000$; Fig. 6b, $t = 10000$. Fig. 6c: the maximum, average, minimum value of S (susceptible) with time increasing from $t = 0$ to $t = 10000$. Fig. 6d: the three-dimensional sketch pattern at $t = 10000$.

6. Conclusion

This work firstly divides the population into three groups: susceptible individuals (S), infectious individuals (I), and removed individuals (R). Then we propose a rumor propagation dynamic model with Allee effect and cross-diffusion. In this model, Allee effect is considered in the growth of population, and a time delay term is added to reflect the delay effect of the environment's restriction on population growth, and the contact term uses high-time exposure saturation. In addition, we have analyzed a general form of cross-diffusion model with time delay, and drawn a general conclusion of linear stability analysis of Turing bifurcation. However, Turing bifurcation analysis cannot give the specific shape of the pattern under certain conditions. The amplitude equation theory states that an ideal pattern without any defects near the bifurcation points of the system can be described by the linear combination of oscillating wave vectors, so that the shapes of the patterns can be predicted. In this part, we use a lot of contents to derive the general expression of the weak nonlinear model amplitude equation via the help of multiple scale analysis. Finally, we apply the above theorems to the analysis of our previously proposed model, and derive the appearance condition of the Turing bifurcation and the expression of the amplitude equation respectively. In the numerical simulation part, we use the amplitude equation theorem to decide the pattern shapes. The influence of time delay and three different network structures on the pattern shapes are also explored. Through numerical simulations, we have verified the correctness of the above theoretical analysis.

We have also tried to transform the reaction–diffusion system with time delay into an approximate system without time delay, and then use the conclusions derived from the amplitude equation to conduct further simulation studies. A common way of transformation is to write Eq. 3.13 in matrix form, and then left-multiply both sides by matrix M. After doing this, the variables S, I, F, G, and the diffusion coefficients d_{ij} all need to be redefined. But at this time, the new S appears in $\partial S/\partial t$ on the

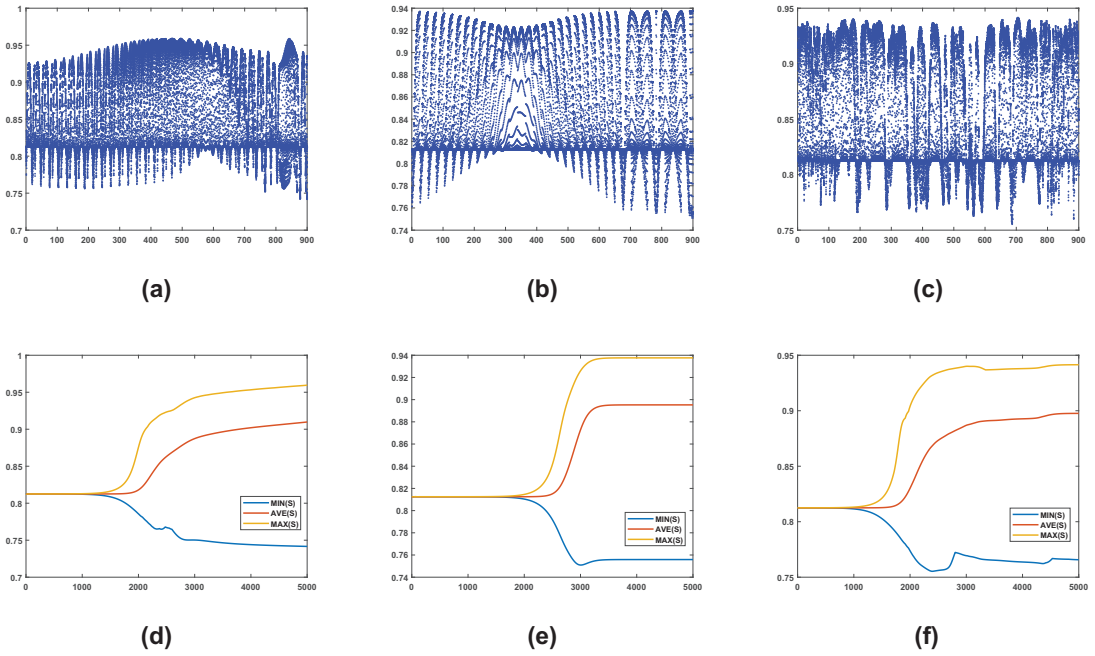

Fig. 7. The value of the control variable is 0.65, and the values of other variables are consistent with those in Fig. 4. The first three pictures show the density of susceptible individuals at each node at $t = 5000$. The network structures represented by each picture are: Fig. 7a, LA4; Fig. 7b, LA12; Fig. 7c, WS. The last three graphs are about the maximum, minimum, and average values for the density of susceptible individuals on the three network structures over time.

left side of the equation, while the old S appears in ΔS on the other side, which is different from the form of the amplitude equation derived in Theorem 4.1. Therefore, in this paper, only the experimental simulation of the amplitude equations without time delay is carried out.

However, how to derive the amplitude equations of the system with time delay is a very valuable topic. We leave it for further work.

Declaration of Competing Interest

The authors declare that they have no known competing financial interests or personal relationships that could have appeared to influence the work reported in this paper.

Acknowledgement

This research is partly supported by National Natural Science Foundation of China (Grant No.12002135, 12102148), China Postdoctoral Science Foundation (Grant No.2019M661732), Natural Science Foundation of Jiangsu Province (CN) (Grant No. BK20190836), Natural Science Research of Jiangsu Higher Education Institutions of China (Grant No.21KJB110010), Jiangsu Province Postdoctoral Science Foundation (Grant No.2021K383C), Young Science and Technology Talents Lifting Project of Jiangsu Association for Science and Technology.

References

[1] Abdelhadi Abta, Hassan Laarabi, Mostafa Rachik, H.T. Alaoui, and Salahaddine Boutayeb. Optimal control of a delayed rumor propagation model with saturated control functions and L^1-type objectives. Social Network Analysis and Mining, 10(1):73, Aug 2020..
[2] W.C. Allee, E.S. Bowen, Studies in animal aggregations: mass protection against colloidal silver among goldfishes, Journal of Experimental Zoology 61 (2) (1932) 185–207.
[3] Malay Banerjee, S. Ghorai, Nayana Mukherjee, Study of cross-diffusion induced turing patterns in a ratio-dependent prey-predator model via amplitude equations, Applied Mathematical Modelling 55 (Mar 2018) 383–399.
[4] Lili Chang, Moran Duan, Guiquan Sun, Zhen Jin, Cross-diffusion-induced patterns in an SIR epidemic model on complex networks. Chaos: An Interdisciplinary, Journal of Nonlinear Science (Jan 2020), 30(1):013147.
[5] Mengxin Chen, Wu. Ranchao, Liping Chen, Spatiotemporal patterns induced by turing and turing-hopf bifurcations in a predator-prey system, Applied Mathematics and Computation (sep 2020), 380:125300.
[6] Shanshan Chen, Haijun Jiang, Liang Li, Jiarong Li, Dynamical behaviors and optimal control of rumor propagation model with saturation incidence on heterogeneous networks, Chaos, Solitons & Fractals 140 (Nov 2020) 110206.
[7] Yingying Cheng, Liang'an Huo, Laijun Zhao, Dynamical behaviors and control measures of rumor-spreading model in consideration of the infected media and time delay, Information Sciences 564 (Jul 2021) 237–253.

[8] G.C. Cruywagen, J.D. Murray, P.K. Maini, Biological pattern formation on two-dimensional spatial domains: a nonlinear bifurcation analysis, SIAM Journal on Applied Mathematics 57 (6) (1997) 1485–1509.
[9] D.J. Daley, D.G. Kendall, Epidemics and rumours, Nature 204 (1118) (1964).
[10] Wenzhen Gan, Peng Zhu, Zuhan Liu, and Canrong Tian. Delay-driven instability and ecological control in a food-limited population networked system. Nonlinear Dynamics, 100(4), 4031–4044, jun 2020..
[11] Zun-Guang Guo, Gui-Quan Sun, Zhen Wang, Zhen Jin, Li Li, Can Li, Spatial dynamics of an epidemic model with nonlocal infection, Applied Mathematics and Computation 377 (Jul 2020) 125158.
[12] Le He, Linhe Zhu, Zhengdi Zhang, Turing instability induced by complex networks in a reaction–diffusion information propagation model, Information Sciences 578 (Nov 2021) 762–794.
[13] Qi Huang, Chuan Zhou, Jia Wu, Luchen Liu, and Bin Wang. Deep spatial-temporal structure learning for rumor detectionon twitter. Neural Computing and Applications, 2020..
[14] Ankur Jain, Joydip Dhar, Vijay Gupta, Rumor model on homogeneous social network incorporating delay in expert intervention and government action, Communications in Nonlinear Science and Numerical Simulation 84 (2020) 105189.
[15] Yoshiki Kuramoto, Toshio Tsuzuki, On the formation of dissipative structures in reaction-diffusion systems: Reductive perturbation approach, Progress of Theoretical Physics 54 (3) (1975) 687–699.
[16] Hassan Laarabi, Abdelhadi Abta, Mostafa Rachik, and Jamal Bouyaghroumni. Stability analysis of a delayed rumor propagation model. Differential Equations and Dynamical Systems, 24(4), 407–415, jun 2015..
[17] Chengxia Lei, Zhigui Lin, Haiyan Wang, The free boundary problem describing information diffusion in online social networks, Journal of Differential Equations 254 (3) (Feb 2013) 1326–1341.
[18] Chunru Li, Zujun Ma, Dynamic analysis of a spatial diffusion rumor propagation model with delay, Advances in Difference Equations 2015 (1) (Nov 2015).
[19] Jiarong Li, Haijun Jiang, Xuehui Mei, Hu. Cheng, Guoliang Zhang, Dynamical analysis of rumor spreading model in multi-lingual environment and heterogeneous complex networks, Information Sciences 536 (Oct 2020) 391–408.
[20] Qiang Li, Zhijun Liu, Sanling Yuan, Cross-diffusion induced turing instability for a competition model with saturation effect, Applied Mathematics and Computation 347 (Apr 2019) 64–77.
[21] Biao Liu, Wu. Ranchao, Liping Chen, Patterns induced by super cross-diffusion in a predator-prey system with michaelis–menten type harvesting, Mathematical Biosciences 298 (Apr 2018) 71–79.
[22] Houye Liu and Weiming Wang. A new mechanical algorithm for calculating the amplitude equation of the reaction-diffusion systems. International Journal of Computational Models and Algorithms in Medicine, 3:21–28, 10 2014..
[23] Hu.a. Liu, Yong Ye, Yumei Wei, Weiyuan Ma, Ming Ma, Kai Zhang, Pattern formation in a reaction-diffusion predator-prey model with weak allee effect and delay, Complexity 2019 (Nov 2019) 1–14.
[24] Wanping Liu, Wu. Xiao, Wu. Yang, Xiaofei Zhu, Shouming Zhong, Modeling cyber rumor spreading over mobile social networks: A compartment approach, Applied Mathematics and Computation 343 (Feb 2019) 214–229.
[25] A.C. Newell, J.A. Whitehead, Finite bandwidth, finite amplitude convection, Journal of Fluid Mechanics 38 (2) (1969) 279–303.
[26] Qi Quyang, Nonlinear Science and the Pattern Dynamics Introduction, Peking University Press, Beijing, 2010.
[27] Xiangyu Tao and Linhe Zhu. Study of periodic diffusion and time delay induced spatiotemporal patterns in a predator-prey system. Chaos, Solitons & Fractals, 150:111101, sep 2021..
[28] A.M. Turing, The chemical basis of morphogenesis, Phil. Trans. R. Soc. Lond. B 237 (641) (1952) 37–72.
[29] Yunpeng Xiao, Diqiang Chen, Shihong Wei, Qian Li, Haohan Wang, Xu. Ming, Rumor propagation dynamic model based on evolutionary game and anti-rumor, Nonlinear Dynamics 95 (1) (Nov 2018) 523–539.
[30] Yu. Shuzhen, Yu. Zhiyong, Haijun Jiang, Jiarong Li, Dynamical study and event-triggered impulsive control of rumor propagation model on heterogeneous social network incorporating delay, Chaos, Solitons & Fractals 145 (Apr 2021) 110806.
[31] Yu. Shuzhen, Yu. Zhiyong, Haijun Jiang, Xuehui Mei, Jiarong Li, The spread and control of rumors in a multilingual environment, Nonlinear Dynamics 100 (3) (Apr 2020) 2933–2951.
[32] Linhe Zhu, Gui Guan, Yimin Li, Nonlinear dynamical analysis and control strategies of a network-based SIS epidemic model with time delay, Applied Mathematical Modelling (jun 2019), 70:512–531.
[33] Linhe Zhu, He. Le, Pattern formation in a reaction-diffusion rumor propagation system with allee effect and time delay, Nonlinear Dynamics 107 (2022) 3041–3063.
[34] Linhe Zhu, Wenshan Liu, Spatial dynamics and optimization method for a network propagation model in a shifting environment, Discrete & Continuous Dynamical Systems - A 41 (4) (2021) 1843–1874.
[35] Linhe Zhu, Mengtian Zhou, Ying Liu, Zhengdi Zhang, Nonlinear dynamic analysis and optimum control of reaction-diffusion rumor propagation models in both homogeneous and heterogeneous networks, Journal of Mathematical Analysis and Applications 502 (2) (Oct 2021) 125260.
[36] Linhe Zhu, Mengtian Zhou, Zhengdi Zhang, Dynamical analysis and control strategies of rumor spreading models in both homogeneous and heterogeneous networks, Journal of Nonlinear Science 30 (6) (May 2020) 2545–2576.